

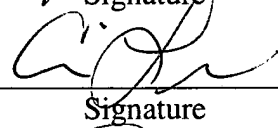
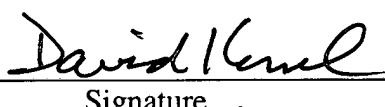
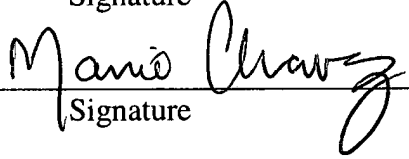
528582

Sandia National Laboratories
Carlsbad Programs Group

Waste Isolation Pilot Plant

A Reconciliation of the CCA and PAVT Parameter Baselines

Revision 3

Author:	Clifford Hansen (6821)		4/11/03
	Print	Signature	Date
Author:	Christi Leigh (6821)		4/11/03
	Print	Signature	Date
Technical Review:	Brian Fox (6821)		4/11/03
	Print	Signature	Date
Management Review:	David Kessel (6821)		4/15/03
	Print	Signature	Date
QA Review:	Mario Chavez (6820)		4/30/03
	Print	Signature	Date

Acknowledgements

Several individuals deserve credit for their substantial contributions to this work. The authors who are primarily responsible for writing and documenting the series of topics are described below:

Frank Hansen (6822)
Disturbed Rock Zone Permeability

Rich Jepsen (6822)
Waste Shear Strength

David Lechel (Lechel Inc.)
Borehole Sand and Borehole Concrete Permeability
Waste Permeability
Effectiveness of Passive Institutional Controls
Drilling Intrusion-Probability of Hitting a Brine Reservoir
Brine Reservoir Parameters

Donald Wall (6821)
Author of Revision 0
Actinide Solubilities
Matrix Distribution Coefficients in the Culebra
Drill String Angular Velocity
Waste Unit Factor

Yifeng Wang (6822)
Inundated Steel Corrosion Rate

TABLE OF CONTENTS

1.	INTRODUCTION	1
2.	BOREHOLE SAND & BOREHOLE CONCRETE PERMEABILITY	4
2.1	INTRODUCTION	4
2.2	BACKGROUND	4
2.3	CCA	4
2.4	PAVT	5
2.5	CONCLUSION	6
3.	DISTURBED ROCK ZONE PERMEABILITY	7
3.1	INTRODUCTION	7
3.2	BACKGROUND	7
3.3	CCA	7
3.4	PAVT	7
3.5	CONCLUSION	8
4.	WASTE PERMEABILITY	8
4.1	INTRODUCTION	8
4.2	BACKGROUND	9
4.3	CCA	9
4.4	PAVT	9
4.5	CONCLUSION	10
5.	EFFECTIVENESS OF PASSIVE INSTITUTIONAL CONTROLS	11
5.1	INTRODUCTION	11
5.2	BACKGROUND	11
5.3	CCA	12
5.4	PAVT	13
5.5	CONCLUSION	15
6.	WASTE SHEAR STRENGTH	15
6.1	INTRODUCTION	15
6.2	BACKGROUND	15
6.3	CCA	16
6.4	PAVT	16
6.5	CONCLUSION	17
7.	ACTINIDE SOLUBILITIES	18
7.1	INTRODUCTION	18
7.2	BACKGROUND	18
7.3	CCA	19
7.4	PAVT	19
7.5	CONCLUSION	20
8.	INUNDATED STEEL CORROSION RATE	21
8.1	INTRODUCTION	21
8.2	BACKGROUND	21

8.3	CCA.....	21
8.4	PAVT	21
8.5	CONCLUSION	22
9.	MATRIX DISTRIBUTION COEFFICIENTS IN THE CULEBRA.....	22
9.1	INTRODUCTION.....	22
9.2	BACKGROUND.....	23
9.3	CCA.....	23
9.4	PAVT	24
9.5	CONCLUSION	24
10.	DRILLING INTRUSION – PROBABILITY OF HITTING A BRINE RESERVOIR.....	25
10.1	INTRODUCTION.....	25
10.2	BACKGROUND.....	25
10.3	CCA.....	26
10.4	PAVT	27
10.5	CONCLUSION	28
11.	DRILL STRING ANGULAR VELOCITY.....	29
11.1	INTRODUCTION.....	29
11.2	BACKGROUND.....	29
11.3	CCA.....	29
11.4	PAVT	30
11.5	CONCLUSION	30
12.	BRINE RESERVOIR PARAMETERS	31
12.1	INTRODUCTION.....	31
12.2	BACKGROUND.....	31
12.3	CCA.....	32
	12.3.1 Brine Reservoir Rock Compressibility.....	32
	12.3.2 Brine Reservoir Pore Volume.....	33
12.4	PAVT	34
	12.4.1 Brine Reservoir Rock Compressibility.....	34
	12.4.2 Brine Reservoir Pore Volume.....	34
12.5	CONCLUSION	35
13.	WASTE UNIT FACTOR.....	36
13.1	INTRODUCTION.....	36
13.2	BACKGROUND.....	36
13.3	CCA.....	37
13.4	PAVT	37
13.5	CONCLUSION	37
14.	REFERENCES.....	39

LIST OF TABLES

Table 1.1. Summary of CCA and PAVT Parameters	2
Table 1.2. Summary of RPB Values and Distributions	3
Table 2.1. Log of Long-term Borehole and Borehole Plug Permeability in CCA and PAVT	6
Table 2.2. Long-term Borehole and Borehole Plug Permeability Parameters in the RPB	6
Table 3.1. DRZ Permeability Parameters in CCA and PAVT	8
Table 3.2. DRZ Permeability Parameters in the RPB.....	8
Table 4.1. Waste Permeability Parameters in CCA and PAVT.....	10
Table 4.2. Waste Permeability Parameters in the RPB	11
Table 5.1 Multiplicative Factor for Passive Institutional Controls in CCA and PAVT.....	15
Table 5.2. Effectiveness of Passive Institutional Controls in the RPB	15
Table 6.1. Waste Shear Strength in CCA and PAVT	17
Table 6.2. Waste Shear Strength in the RPB.....	18
Table 7.1. Definition of the SOLMOD and SOLSIM Parameters.....	18
Table 7.2. Actinide Solubility Parameters Used in the CCA and PAVT	20
Table 7.3. Actinide Solubility Parameters in the RPB.....	20
Table 8.1. Inundated Steel Corrosion Rate in CCA and PAVT	22
Table 8.2. Inundated Steel Corrosion Rate in the RPB	22
Table 9.1. Definition of the Matrix Distribution Parameters.....	23
Table 9.2. Matrix Distribution Coefficient Ranges and Distributions in the CCA	23
Table 9.3. Matrix Distribution Coefficient Ranges and Distributions in the RPB.....	24

Table 10.1. Probability of Hitting a Brine Pocket in CCA and PAVT 28

Table 10.2. Probability of Hitting a Brine Pocket in the RPB 29

Table 11.1. Drill String Angular Velocity in the CCA and PAVT..... 30

Table 11.2. Drill String Angular Velocity in the RPB..... 30

Table 12.1. Brine Reservoir Parameters in the CCA and PAVT..... 35

Table 12.2. Brine Reservoir Parameters in the RPB..... 35

Table 13.1. Radionuclide Release Limits from 40 CFR 191 36

Table 13.2. WIPP Radionuclide Inventory from the CCA..... 37

**Table 13.3. Additional Inventory Contributions from the Savannah River
Site** 38

ACRONYMS

AIC	Active Institutional Controls
BLM	Bureau of Land Management
CFR	Code of Federal Regulations
CCA	Compliance Certification Application
DOE	U.S. Department of Energy
DBR	Direct Brine Release
DRZ	Disturbed Rock Zone
EEG	Environmental Evaluation Group
ETC	Earth Technology Corporation
EPA	U.S. Environmental Protection Agency
FMT	Fracture-Matrix Transport
K_d	Matrix Distribution Coefficient
PA	Performance Assessment
PAVT	Performance Assessment Verification Test
PIC	Passive Institutional Controls
RPB	Reconciled Parameter Baseline
SRS	Savannah River Site
TRU	Transuranic Waste
TWBIR	Transuranic Waste Baseline Inventory Report
WIPP	Waste Isolation Pilot Plant
WPO	WIPP Program Office

PARAMETERS ADDRESSED IN THIS REPORT

Material Name	Property Name	Section
BH_SAND	PRMX_LOG	2
BH_SAND	PRMY_LOG	
BH_SAND	PRMZ_LOG	
CONC_PLG	PRMX_LOG	2
CONC_PLG	PRMY_LOG	
CONC_PLG	PRMZ_LOG	
DRZ_1	PRMX_LOG	3
DRZ_1	PRMY_LOG	
DRZ_1	PRMZ_LOG	
WAS_AREA	PRMX_LOG	4
WAS_AREA	PRMY_LOG	
WAS_AREA	PRMZ_LOG	
GLOBAL	FPICD	5
GLOBAL	FPICM	
BOREHOLE	TAUFAIL	6
SOLMOD3	SOLSIM	7
	SOLCIM	
SOLMOD4	SOLSIM	
	SOLCIM	
SOLMOD5	SOLSIM	
	SOLCIM	
STEEL	CORRMCO2	8
AM+3	MKD_AM	9
NP+4	MKD_NP	
NP+5	MKD_NP	
PU+3	MKD_PU	
PU+4	MKD_PU	
TH+4	MKD_TH	
U+4	MKD_U	
U+6	MKD_U	
GLOBAL	PBRINE	10
BOREHOLE	DOMEGA	11
CASTILER	COMP_RCK	12
CASTILER	POR_BPKT	12
BOREHOLE	WUF	13

PERFORMANCE ASSESSMENT CODES ADDRESSED IN THIS REPORT

Code	Description
BRAGFLO	A two-phase flow code that simulates gas and brine flow as well as incorporates the effects of disposal room consolidation and closure, gas generation, and interbed fracture in response to gas pressure.
CCDFGF	A code that assembles results from calculations performed with the other PA codes into the CCDF specified in 40 CFR 191. It implements a Monte Carlo CCDF construction.
CUTTINGS_S	A multi-faceted computational procedure that assesses the effects of direct removal of wastes.
FMT	Solves chemical equilibrium problems using the Pitzer activity coefficient formalism.
LHS	A Latin Hypercube sampling code designed to sample the entire range of variability of all uncertain parameters.
NUTS	Calculates radionuclide transport based on flows and saturations calculated by BRAGFLO
PANEL	Calculates in-solution radionuclide source term for WIPP PA, accounting for radioactive decay and radionuclide solubilities
SECOTP2D	Calculates radionuclide transport in the Culebra based on flows to the Culebra calculated by BRAGFLO

This page left intentionally blank

1. INTRODUCTION

In 1996 the Department of Energy (DOE) completed a performance assessment (PA) calculation for the Waste Isolation Pilot Plant (WIPP.) The PA was part of the Compliance Certification Application (CCA) submitted to the Environmental Protection Agency (EPA) to demonstrate compliance with the radiation protection regulations of 40 CFR 191 and 40 CFR 194. The calculation used a large number of parameters as inputs to computer models that calculated the evolution of various physical processes, such as brine and gas flow in the repository. The values of many parameters were uncertain; consequently, parameter values for calculations were sampled from appropriate distributions.

In 1997, the EPA required a verification of the calculations done for the CCA, termed the Performance Assessment Verification Test (PAVT). In its review of the CCA, the EPA identified a subset of the CCA parameters whose values and distributions were in question (EPA, 1998a). EPA then required that DOE use revised parameters in a new PA calculation (the PAVT calculation) that subsequently became part of the WIPP's regulatory basis. Consequently, EPA's approval of the CCA was based on two PA calculations, which were based on two different sets of parameters.

As required by the WIPP Land Withdrawal Act, DOE is required to submit documentation to EPA for the recertification of the WIPP every five years. In support of the recertification submittal scheduled for 2003, DOE proposes to reconcile the parameter sets used for the CCA and the PAVT and establish a single parameter set termed the Reconciled Parameter Baseline (RPB). The RPB is the first step in a process that will lead to a single parameter database for recertification calculations, reducing costs and simplifying EPA's review of DOE's recertification application.

The CCA and PAVT calculations involved more than 1500 parameters as inputs to the PA computer codes. For all but 23 of these parameters the values and distributions in the CCA and PAVT are the same. Thus, the RPB consists primarily of parameters where the CCA and PAVT agree.

This document details those parameters where the CCA and PAVT differ. The document re-examines supporting documentation for the CCA and the PAVT and consider the results of more recent research. For each parameter, the document summarizes rationale for the ranges and distributions used in each calculation and recommends a range and value for the RPB. With few exceptions the RPB adopts the parameter values and distributions from the PAVT. Table 1.1 lists the parameters of interest along with the CCA and PAVT values. Table 1.2 lists the RPB values and distributions for the parameters of interest.

Table 1.1. Summary of CCA and PAVT Parameters

Parameter	CCA Range and Distribution	PAVT Range and Distribution
Log of Borehole Sand Permeability	-14 to -11 log m ² Uniform	-16.3 to -11 log m ² Uniform
Borehole Concrete Permeability	-16.3 log m ² Constant	10 ⁻¹⁹ to 10 ⁻¹⁷ m ² Uniform
Log of Disturbed Rock Zone Permeability	-15 log m ² Constant	-19.4 to -12.5 log m ² Uniform
Log of Waste Permeability	-12.769 log m ² Constant	-12.6198 log m ² Constant
PIC Reduction Factor for 100 – 700 years	0.01 Constant	1.0 Constant
Waste Shear Strength	0.05 to 10 Pa Uniform	0.05 to 77 Pa Loguniform
Coefficient, A, in Equation ^(a) for Solubility for Am(III) and Pu(III) in Castile Brine	6.52 x 10 ⁻⁸ mol/l constant	1.3 x 10 ⁻⁸ mol/l constant
Coefficient, A, in Equation ^(a) for Solubility for Np+4, Pu(IV), Th(IV) and U(IV) in Castile Brine	6.0 x 10 ⁻⁹ mol/l constant	4.1 x 10 ⁻⁸ mol/l constant
Coefficient, A, in Equation ^(a) for Solubility for Np(V) in Castile Brine	2.2 x 10 ⁻⁶ mol/l constant	4.8 x 10 ⁻⁷ mol/l constant
Coefficient, A, in Equation ^(a) for Solubility for Am(III) and Pu(III) in Salado Brine	5.82 x 10 ⁻⁷ mol/l constant	1.2 x 10 ⁻⁷ mol/l constant
Coefficient, A, in Equation ^(a) for Solubility for Np(IV), Pu(IV), Th(IV) and U(IV) in Salado Brine	4.4 x 10 ⁻⁶ mol/l constant	1.3 x 10 ⁻⁸ mol/l constant
Coefficient, A, in Equation ^(a) for Solubility for Np(V) in Salado Brine	2.3 x 10 ⁻⁶ mol/l constant	2.4 x 10 ⁻⁷ mol/l constant
Inundated Steel Corrosion Rate	0 to 1.59x10 ⁻¹⁴ m/s Uniform	0 to 3.17x10 ⁻¹⁴ m/s Uniform
K _d in Culebra Dolomite for Am(III) and Pu(III)	0.02 to 0.5 m ³ /kg Uniform	0.02 to 0.5 m ³ /kg Loguniform
K _d in Culebra Dolomite for Np(IV), Pu(IV), Th(IV), and U(IV)	0.9 to 20 m ³ /kg Uniform	0.9 to 20 m ³ /kg Loguniform
K _d in Culebra Dolomite for Np(V)	0.001 to 0.2 m ³ /kg Uniform	0.001 to 0.2 m ³ /kg Loguniform
K _d in Culebra Dolomite for U(VI)	0.00003 to 0.03 m ³ /kg Uniform	0.00003 to 0.03 m ³ /kg Loguniform
Probability of Hitting a Brine Pocket	0.08 Constant	0.01 to 0.60 Uniform
Drill String Angular Velocity	7.8 radians/s Constant	4.2 to 23.0 radians/s cumulative distribution with mean of 7.77 radians/s
Castile Brine Pocket Rock Compressibility	Min: -11.3 log Pa ⁻¹ Max: -8 log Pa ⁻¹ Mode: -10 log Pa ⁻¹ Triangular	Min: 2x10 ⁻¹¹ Pa ⁻¹ Max: 1x10 ⁻¹⁰ Pa ⁻¹ Mode: 4x10 ⁻¹¹ Pa ⁻¹ Triangular
Castile Brine Pocket Porosity	Not used in CCA	Min: 0.1848; Max: 0.9240; Mode 0.3696 Triangular
Brine Pocket Pore Volume	(3.2, 6.4, 9.6, 12.8, 16) x 10 ⁴ m ³ Discrete	Calculated from Brine Pocket Porosity
Inventory Waste Unit Factor	4.07 Constant	3.44 Constant

^(a)The equation for solubility is $A \cdot 10^b$ where b is a sampled value. Only the coefficient, A , was changed in the PAVT.

Table 1.2. Summary of RPB Values and Distributions

Parameter	Range	Distribution
Log of Borehole Sand Permeability	-16.3 to -11 log m ²	Uniform
Log of Borehole Concrete Permeability	-19 to -17 log m ²	Uniform
Log of Disturbed Rock Zone Permeability	-19.4 to -12.5 log m ²	Uniform
Log of Waste Permeability	-12.6198 log m ²	Constant
PIC Reduction Factor for 100 – 700 years	1.0	Constant
Waste Shear Strength	0.05 to 77 Pa	Loguniform
Coefficient, A, in Equation ^(a) for Solubility for Am(III) and Pu(III) in Castile Brine	1.3 x 10 ⁻⁸ mol/l	Constant
Coefficient, A, in Equation ^(a) for Solubility for Np(IV), Pu(IV), Th(IV) and U(IV) in Castile Brine	4.1 x 10 ⁻⁸ mol/l	Constant
Coefficient, A, in Equation ^(a) for Solubility for Np(V) in Castile Brine	4.8 x 10 ⁻⁷ mol/l	Constant
Coefficient, A, in Equation ^(a) for Solubility for Am(III) and Pu(III) in Salado Brine	1.2 x 10 ⁻⁷ mol/l	Constant
Coefficient, A, in Equation ^(a) for Solubility for Np(IV), Pu(IV), Th(IV) and U(IV) in Salado Brine	1.3 x 10 ⁻⁸ mol/l	Constant
Coefficient, A, in Equation ^(a) for Solubility for Np(V) in Salado Brine	2.4 x 10 ⁻⁷ mol/l	Constant
Inundated Steel Corrosion Rate	0 to 3.17x10 ⁻¹⁴ m/s	Uniform
K _d in Culebra Dolomite for Am(III) and Pu(III)	0.02 to 0.4 m ³ /kg	Loguniform
K _d in Culebra Dolomite for Np(IV), Pu(IV), Th(IV), and U(IV)	0.7 to 10 m ³ /kg	Loguniform
K _d in Culebra Dolomite for Np(V)	0.001 to 0.2 m ³ /kg	Loguniform
K _d in Culebra Dolomite for U(VI)	0.00003 to 0.02 m ³ /kg	Loguniform
Probability of Hitting a Brine Pocket	0.01 to 0.60	Uniform
Drill String Angular Velocity	4.2 to 23.0 radians/sec	Cumulative distribution based on range with mean value of 7.77 radians/s
Castile Brine Pocket Rock Compressibility	Min: 2x10 ⁻¹¹ Pa ⁻¹ Max: 1x10 ⁻¹⁰ Pa ⁻¹ Mode 4x10 ⁻¹¹ Pa ⁻¹	Triangular
Castile Brine Pocket Porosity	Min: 0.1848; Max: 0.9240; Mode 0.3696	Triangular
Brine Pocket Pore Volume	Calculated from Brine Pocket Porosity	Not applicable
Inventory Waste Unit Factor	3.59	Constant

^(a)The equation for solubility is $A \cdot 10^b$ where b is a sampled value. Only the coefficient, A, was changed in the PAVT.

2. BOREHOLE SAND & BOREHOLE CONCRETE PERMEABILITY

2.1 INTRODUCTION

This section documents the type of distribution and range of values selected for the borehole sand and borehole concrete permeability in the RPB. These parameters are implemented as PRMX_LOG, PRMY_LOG, and PRMZ_LOG for the materials BH_SAND and CONC_PLG. PRMX_LOG, PRMY_LOG, and PRMZ_LOG are the logarithms of permeability in the x-, y-, and z-directions, respectively, and are used in the BRAGFLO code.

2.2 BACKGROUND

Long-term releases to the ground surface or into groundwater in the Rustler or overlying units in the vicinity of WIPP may occur through borehole intrusions into the repository. The disturbed-performance, deep-drilling scenarios used in PA involve at least one deep-drilling event that intersects the waste disposal region. According to specific guidance provided by the EPA (section 194.33 of EPA, 1998b), DOE's analysis of the consequences of future drilling events assumes that:

- Future drilling practices and technology will remain consistent with those in use in the Delaware Basin (where the WIPP is located) at the time a compliance application is prepared, and
- Natural processes will govern the capability of boreholes to transmit fluids over the regulatory time frame.

With EPA's guidance in mind, the DOE evaluated the procedures that are currently used to plug boreholes in standard oil-field operations within the controlled area around the WIPP and developed a set of assumptions for the deep-drilling scenarios for PA. The DOE's evaluation included an investigation of the types and amounts of drilling fluids used, the borehole depths, the borehole diameters, the borehole seal materials, and the fraction of such boreholes that are sealed by humans. As a result of their investigations, DOE assumed that in the future shallow boreholes would be plugged as they are now, in accordance with current state or federal regulations using materials shown to be compatible with the underground environment (DOE, 1996a).

2.3 CCA

In preparation for the CCA, DOE developed a set of assumed plug configurations for boreholes drilled and abandoned in the future. Each assumed plug configuration involves several materials with varying degrees of integrity over the lifetime of the repository. One material used in the CCA PA borehole models is a concrete material. DOE assumed that initially, the concrete plugs would be effective in limiting fluid flow in the borehole. However, for purposes of the CCA PA calculation, some plugs above the repository were assumed to degrade after 200 years of emplacement. From that point on, the borehole was assumed to be filled with a silty, sand-like material containing degraded concrete, corrosion products resulting from degradation of the casing, and material that sloughs off of the walls of the borehole.

In the CCA, borehole concrete permeability was set at a constant $5 \times 10^{-17} \text{ m}^2$, based on results reported by Thompson et al. (1996). This value was directly measured for a concrete borehole plug at the WIPP site (Christensen and Hunter, 1980).

Borehole sand permeability was given values representative of the intrinsic permeability of a silty, sandy material, ranging from 10^{-14} to 10^{-11} m^2 . This permeability range is representative of a mix of degraded concrete, corroded steel borehole casing, and material which may slough into the borehole or spall from the walls of the borehole over time (see Freeze and Cherry, 1979). Because of the uncertainty in the permeability of this composite material, the CCA used a distribution of values where the log of the permeability has a uniform distribution over the range of -14 to -11.

2.4 PAVT

In the PAVT, EPA required the DOE to consider a range of values for the borehole concrete permeability. The lower bound of the range chosen by EPA, $1 \times 10^{-19} \text{ m}^2$, is more than two orders of magnitude lower than the lowest value measured for a WIPP borehole plug grout ($5 \times 10^{-17} \text{ m}^2$) as reported by Christensen and Hunter (1980). EPA considered this to be a more conservative lower bound because a less permeable borehole plug may result in higher repository gas pressures and hence greater releases during a human intrusion event. EPA chose an upper bound, $1 \times 10^{-17} \text{ m}^2$, that was equal to the permeability of the concrete in the shaft seal systems. At the time of the PAVT calculations, the EPA specified a uniform distribution over the permeability range (from 10^{-19} to 10^{-17}). (Froehlich, 1997)

EPA also questioned the range of borehole sand permeabilities and the assumption that concrete borehole plugs would degrade to a more permeable material. EPA (EPA, 1997a) concluded that the lower bound for long-term borehole sand permeability proposed by DOE (10^{-14} m^2) should be closer to that of an undegraded borehole plug ($5 \times 10^{-17} \text{ m}^2$). The lower value was of interest to EPA because a lower permeability could result in increased gas pressures with consequent increases in brine and spallings releases during a human intrusion event.

Like DOE, the EPA investigated drilling practices used in the petroleum industry and found literature values for cement permeability ranging from 9×10^{-21} to $1 \times 10^{-16} \text{ m}^2$ (EPA, 1997b). The EPA also found that filter cake and compacted, clay-based drilling muds can yield permeabilities of less than $9.9 \times 10^{-22} \text{ m}^2$. In their considerations, the EPA noted that drilling mud used in the Delaware Basin boreholes may not have the permeability of clay-based solids; however, they noted that natural cuttings could contribute to lower borehole permeabilities than those assumed by the DOE. The EPA also postulated that the effective average permeability over an abandoned borehole could remain in the range of 9×10^{-21} to $1 \times 10^{-16} \text{ m}^2$ over a period of hundreds of years or more if complete degradation does not occur throughout a plug configuration or if natural materials or mud were to provide additional layers with sealing properties.

With these findings, the EPA decided that the borehole sand permeabilities assigned by DOE in its CCA, while consistent with the broad range of available data, did not adequately represent the total range of permeability conditions that could exist. As a result, EPA required DOE to

perform simulations with lower borehole sand permeabilities as shown in Table 2.1.

Table 2.1. Log of Long-term Borehole and Borehole Plug Permeability in CCA and PAVT

Parameter Identifier ^(a)	CCA Value	PAVT Value
CONC_PLG/PRMX_LOG CONC_PLG/PRMY_LOG CONC_PLG/PRMZ_LOG	-16.3 Constant	Parameter name changed for the PAVT
CONC_PLG/PRMX CONC_PLG/PRMY CONC_PLG/PRMZ	N/A	10 ⁻¹⁹ to 10 ⁻¹⁷ Uniform Distribution
BH_SAND/PRMX_LOG BH_SAND/PRMY_LOG BH_SAND/PRMZ_LOG	-14 to -11 Uniform	-16.3 to -11 Uniform

^(a)The material name is listed first followed by the property name.

Subsequent to the completion of the PAVT, the EPA produced a series of Technical Support Documents (TSD) to document their review of the CCA. In these TSDs, the EPA specified a uniform distribution for the log of the borehole concrete permeability, rather than a uniform distribution for the borehole concrete permeability. (EPA, 1998a) The range of permeabilities specified in the TSD is the same as the range used in the PAVT calculations.

2.5 CONCLUSION

The Sandia National Laboratories Technical Library and Records Center undertook a literature and records search to identify recent research that addresses the permeability of borehole sand and borehole concrete. No new information was found that directly addressed borehole permeabilities. Sandia National Laboratories chose the distribution specified in the TSD for the permeability of the concrete borehole plug rather than that used in the PAVT calculations. The RPB borehole sand and borehole concrete permeabilities will be as shown in Table 2.2.

Table 2.2. Long-term Borehole and Borehole Plug Permeability Parameters in the RPB

Parameter Description	Parameter Identifier ^(a)	Range	Distribution
Log of Borehole Concrete Permeability	CONC_PLG/PRMX_LOG CONC_PLG/PRMY_LOG CONC_PLG/PRMZ_LOG	-19 to -17	Uniform
Log of Borehole Sand Permeability	BH_SAND/PRMX_LOG BH_SAND/PRMY_LOG BH_SAND/PRMZ_LOG	-16.3 to -11	Uniform

^(a)The material name is listed first followed by the property name.

3. DISTURBED ROCK ZONE PERMEABILITY

3.1 INTRODUCTION

This section documents the type of distribution and range of values selected for the permeabilities of the Disturbed Rock Zone (DRZ) in the RPB. These parameters are implemented as PRMX_LOG, PRMY_LOG, and PRMZ_LOG for the material DRZ_1. PRMX_LOG, PRMY_LOG, and PRMZ_LOG are the logarithms of permeability in the x-, y-, and z-directions, respectively, and are used in the BRAGFLO code.

3.2 BACKGROUND

In the DRZ near the repository, permeability and porosity are expected to generally increase in both halite and interbeds due to a variety of processes. Creep closure and stress-field alterations as the result of the excavation are the dominant causes. The increases in permeability and porosity in the interbeds are not expected to be completely reversible with creep closure of the disposal rooms. The increase in DRZ permeability increases the ability of fluid to flow from interbeds to the waste disposal region. The increase in DRZ porosity provides a volume in which some fluid could be retained preventing it from contacting waste or slowing the transport of actinides in solution. Dilation initiates upon excavation and microfractures are created by stress differences. Although stresses tend to decrease in a creeping medium, such as rock salt, the fractures continue to grow and coalesce in an arching pattern around the drifts, and are preferentially oriented parallel to the opening. The DRZ is also reversible in salt. When a rigid plug, such as the panel closure concrete, is placed in a drift, the impinging salt experiences a "back-stress", which reduces stress differences. As the state of stress approaches equilibrium, existing microfractures heal. The DRZ around the panel closure concrete will be rapidly healed. By contrast, the DRZ around rooms would continue to evolve until the country rock compresses the waste stack. Eventually, the entire repository will be entombed by the salt.

The DRZ can be observed today in the underground at WIPP, and permeability measurements have been made. Permeability values and geometrical extent of the DRZ are based on observations, measurements and an understanding of the mechanical response.

3.3 CCA

The grid used in CCA calculations implemented a DRZ of constant permeability (10^{-15} m^2) over a region 12 m above and 2.23 m below the disposal rooms. The grid was continuous above panel closure systems, such that the same permeability and thickness existed above and below the simulated panel closures. A more realistic representation of the DRZ over disposal rooms would include high permeability near the free surface of rooms, and reduction of permeability as a function of depth into the surrounding rock. Generally speaking, the DRZ extends greater distances above a room than below, and is relatively shallow into the ribs.

3.4 PAVT

The EPA determined an alternate lower bound for DRZ permeability from measured gas permeability in anhydrite cores from Marker Bed 139 (Howarth, 1996; Beauheim, 1996, Howarth

and Christain-Frear, 1994). The EPA concluded that a value of -19.4 for the log of the permeability was a more appropriate lower bound for the range of likely values. The EPA selected a value of -12.5 as an upper bound on the log of DRZ permeability based upon a sensitivity analysis (EPA, 1998a). The EPA also assigned a uniform distribution for the range of -19.4 to -12.5 based on the supposition that all the values are equally likely. The geometric dimensions of the DRZ are the same in the CCA and the PAVT. Table 3.1 summarizes the changes made between the CCA and the PAVT.

Table 3.1. DRZ Permeability Parameters in CCA and PAVT

Parameter Identifier ^(a)	CCA Value	PAVT Value
DRZ_1/PRMX_LOG DRZ_1/PRMY_LOG DRZ_1/PRMZ_LOG	Log of the DRZ permeability was a constant value of -15	Log of the DRZ permeability was changed to a uniform distribution ranging from -19.4 to -12.5.

^(a)The material name is listed first followed by the property name.

3.5 CONCLUSION

Documents held by the WIPP Project Office (WPO) pertaining to DRZ permeability values support the magnitude and range of the PAVT values. Beauheim (1996) includes one data set comprising 14 tests, which yields a permeability range from 10^{-21} to $10^{-12.5}$ m². Beauheim (1996) references other data packages that include laboratory measurements on Marker Bed 139 anhydrite. From a total of 42 anhydrite samples, a pressure-sensitive permeability from 10^{-21} to 10^{-16} m² was reported. We conclude that the range employed in the PAVT is appropriate based on these data. Therefore, in the RPB the log of the DRZ permeability will be as shown in Table 3.2.

Table 3.2. DRZ Permeability Parameters in the RPB

Parameter Description	Parameter Identifier ^(a)	Range	Distribution
Log of DRZ Permeability	198 - DRZ_1/PRMX_LOG 199 - DRZ_1/PRMY_LOG 200 - DRZ_1/PRMZ_LOG	-19.4 to -12.5	Uniform

^(a)The material name is listed first followed by the property name.

4. WASTE PERMEABILITY

4.1 INTRODUCTION

This section documents the type of distribution and range of values selected for the permeabilities of the emplaced waste in the RPB. These parameters are implemented as PRMX_LOG, PRMY_LOG, and PRMZ_LOG for the material WAS_AREA. PRMX_LOG, PRMY_LOG, and PRMZ_LOG are the logarithms of permeability in the x-, y-, and z-directions, respectively, and are used in the BRAGFLO code.

4.2 BACKGROUND

Fluid flow modeling within the repository is concerned with (1) fluid flow within the repository (2) fluid flow between the repository and the Salado, the shafts, and intrusion boreholes. Fluid flow results are required to properly estimate releases of radionuclides from the disposal system. Waste permeability significantly affects flow rates of gas and brine. Because the waste disposal region is confined between layers of intact halite characterized by very low permeabilities (less than 10^{-21} m^2), the waste and the surrounding DRZ are the dominant paths for fluid flow within the repository in both the undisturbed and disturbed scenarios.

4.3 CCA

For the CCA, the DOE assumed homogenous material properties for the waste. Further, because of the rate of creep closure, the DOE believed that the waste would reach a "final" compacted condition within a relatively short period after closure. Thus, DOE treated waste permeability as a constant (in BRAGFLO) having a value of $1.7 \times 10^{-13} \text{ m}^2$ in the CCA.

DOE considered the results of laboratory tests on different material groups to determine the overall waste permeability value used in the CCA. In these tests, DOE used the likely composition of wastes destined for disposal (Butcher, 1989) to select different mixtures of surrogate materials for evaluation. Materials were saturated in brine and compacted under stress equivalent to that which would be experienced at repository depth. Brine permeabilities of the waste were determined by establishing a constant flow rate through the surrogate samples and then measuring flow rate and pressure drop (see Thompson and Luker, 1990 for an explanation of the material composition and test procedures).

As expected, permeabilities varied with the material mixtures. Most waste materials exhibited permeabilities of about 10^{-14} to 10^{-13} m^2 (Luker et al., 1991). Granular material mixtures ranged from about 10^{-13} to 10^{-12} m^2 , while mixtures of crushed salt and metals varied from 10^{-14} to more than 10^{-12} m^2 . For all materials tested, permeabilities ranged from 10^{-16} to 10^{-12} m^2 . Based on this range, DOE determined that a value of $1.7 \times 10^{-13} \text{ m}^2$ (log value of -12.769) represented the average permeability of compacted waste, and this value was used in the CCA.

DOE also determined that a constant value was appropriate. The basis for this determination can be found in Vaughn et al. (1995).

4.4 PAVT

EPA, in its review of the CCA and other documentation, questioned the waste permeability value assigned by DOE and required that a value of $2.4 \times 10^{-13} \text{ m}^2$ be used in the PAVT. EPA selected this value based on the results of the peer review conducted by DOE and included in the CCA (DOE, 1996a).

The DOE-sponsored peer review found that Sandia National Laboratories (Sandia WIPP, 1991) generated median waste permeabilities for three types of transuranic waste: combustibles, metals and glass, and sludges. These values were compared with data derived by Butcher (1990) and

Luker et al. (1991). It was posited (Sandia WIPP, 1991) that the distribution of permeability of a collapsed drum would be the weighted sum of the permeability distributions for the waste components, modeled as uniform distributions and weighted by the percent by volume of each component. Based on an anticipated transuranic waste composition of 40% combustibles, 40% metals and glass, and 20% sludges, the expected permeability was recalculated and found to be $2.1 \times 10^{-13} \text{ m}^2$.

Upon further review, Sandia National Laboratories (Tierney, 1990) determined that the waste component permeability distributions would be better modeled by piecewise-linear cumulative distributions rather than uniform distributions. Using these revised distributions, the mean values for the permeability of combustibles, metals/glass, and sludges were calculated to be 5.9×10^{-14} , 5.5×10^{-13} , and $1.05 \times 10^{-16} \text{ m}^2$, respectively. These permeabilities were combined and weighted by the volume of each waste component to obtain a value for waste permeability of $2.4 \times 10^{-13} \text{ m}^2$.

Based on this peer review, EPA concluded that the appropriate value for waste permeability for inclusion in the PAVT should be $2.4 \times 10^{-13} \text{ m}^2$ (EPA, 1998a and b). EPA considered this change minor, and it was made primarily to correct a computational error as opposed to modifying a concept. Furthermore, the PAVT value was found by the peer review panel to be appropriate when compared with permeabilities of compacted municipal landfill waste. The peer review panel also noted that uncertainties could cause waste permeability to vary. However, EPA concluded that since the waste permeability value is more than two orders of magnitude higher than that of any other geologic or seal component, flow through the waste would be relatively fast and long-term releases from the repository would be relatively insensitive to changes in waste permeability.

Table 4.1 lists the values for the log of the waste permeability in the CCA and the PAVT.

Table 4.1. Waste Permeability Parameters in CCA and PAVT

Parameter Identifier ^(a)	CCA Value	PAVT Value
WAS_AREA/PRMX_LOG WAS_AREA/PRMY_LOG WAS_AREA/PRMZ_LOG	A constant value for the log of the waste permeability of -12.769 was used	Log of the waste permeability was changed to a constant value of -12.6198

^(a)The material name is listed first followed by the property name.

4.5 CONCLUSION

The Sandia National Laboratories Technical Library and Records Center undertook a key word-based (waste permeability) literature and records search to identify documentation/research that addresses the parameter, waste permeability. Titles of all recent documents identified by the search were reviewed for relevancy; following this, abstracts and/or complete documents were reviewed to determine if information more recent than that cited in the CCA or PAVT was available. The literature and records search and review did not identify new information that would offer further support of, or otherwise refute the PAVT value of $2.4 \times 10^{-13} \text{ m}^2$ for waste permeability. Therefore, the waste permeability in the RPB will be the same as in the PAVT, as

shown in Table 4.2.

Table 4.2. Waste Permeability Parameters in the RPB

Parameter Description	Parameter Identifier ^(a)	Range	Distribution
Log of Waste Permeability	WAS_AREA/PRMX_LOG WAS_AREA/PRMY_LOG WAS_AREA/PRMZ_LOG	-12.6198	Constant

^(a)The material name is listed first followed by the property name.

5. EFFECTIVENESS OF PASSIVE INSTITUTIONAL CONTROLS

5.1 INTRODUCTION

This section documents the type of distribution and range of values selected for the Passive Institutional Controls (PIC) multiplicative factor that is applied to the frequency of WIPP human intrusion by drilling and by mining in the RPB. These parameters are implemented as FPICD and FPICM for the material GLOBAL. FPICD and FPICM are factors applied to the frequency of WIPP human intrusion by drilling and mining, respectively, and are used in the CUTTINGS_S code.

5.2 BACKGROUND

Active and passive institutional controls are required by the EPA's disposal rule to deter human activity that may be detrimental to the performance of the WIPP repository. Active institutional controls (AIC) will be established after final facility closure to control access to the site and to preclude mining and human intrusion into the disposal system. EPA, in their regulations (40 CFR § 191.14(a)), establishes a limitation of 100 years for considering the effectiveness of AIC in the performance assessment calculation. Because of the nature of the AIC, DOE assumed in the CCA (Section 6.4.12.1 of DOE, 1996a) that there would be no mining or inadvertent human intrusions into the disposal system for the first 100 years after closure of the repository. Therefore, no changes to the PA baseline will be made concerning the influence of AIC on the disposal system.

Passive institutional controls are intended to function without on-site human support or maintenance to deter inadvertent human intrusion into the disposal system. They are intended to communicate to potential intruders the existence and location of the repository, the waste buried there, the nature of the hazard, and the goal of not disturbing the disposal system. DOE undertook various evaluations to develop a conceptual system of integrated components (e.g., earthen berms, monuments, buried markers, information rooms, records) that comprise the PIC system described in the CCA (Appendix PIC/DOE, 1996a).

DOE also evaluated the potential effectiveness of the PIC system in deterring human intrusion (Appendix EPIC/DOE, 1996a). This evaluation considered existing information and perspectives, developed external to DOE, to:

- Finalize the conceptual models of the PIC system that DOE would commit to implementing in the CCA, and
- Assess the effectiveness of the PIC in reducing the inadvertent intrusion frequency.

EPA, in their preamble to the criteria for certification of WIPP, limits credit for effectiveness of PIC in the performance assessment to 700 years after closure of the facility. EPA also states that DOE may propose to reduce the rate of human intrusion by a fractional amount, extending over a technically supportable period of time, but must justify this by using the plans for the implementation of PIC and associated evidence of their effectiveness.

5.3 CCA

In the CCA, DOE describes a PIC system comprising multiple types and multiple levels of passive controls to make human intrusion into the disposal system less likely. This system includes several types of durable monuments and markers, land ownership, and written notations in land records at numerous locations. Written documentation is to include information on the location, design, and disposal contents and hazards, as well as stipulations on allowable land uses. Components of the PIC system are to be instituted at the site and at remote locations.

DOE undertook, via a PIC Task Force, to develop a numerical representation of the effectiveness of PIC in deterring inadvertent human intrusion into the disposal system. The approach assessed the effectiveness of the PIC by considering historical analogues; a one-to-one comparison was developed between individual PIC and individual historical analogues. At the same time, DOE identified potential failure mechanisms of the marker components, the records and archives system, and governmental control components. DOE believes that physical failure of the PIC over the entire withdrawal area will not occur in the time frame of regulatory interest because the PIC were designed to address failure mechanisms based on historical analogues that endured and those for which there is a record of failure.

After physical durability was evaluated, DOE studied the potential of messages to be understood. Hypotheses were developed about how future societies might operate; these focused on potential exploratory intrusions to explore and exploit nature resources. One of the key assumptions is that English will be understandable to the resources exploration community for at least 1,000 years. This assumption is based on 1,000-year old English literature that can be understood by today's scholars, and that English is a world language with a concomitant inertia against radical and rapid change.

The only failure mode that remained after these evaluations was human error – either in obtaining and documenting a lease or a permit to drill, or in drilling in the wrong location. DOE searched the New Mexico portion of the Delaware Basin resource records and did not find any

documentation of wells drilled in the wrong location. DOE then contacted four individuals experienced in drilling in both the Delaware Basin and the encompassing Permian Basin to determine whether there were instances of drilling in the wrong locations. These individuals could cite only five such instances. Based on the 429,000 wells drilled, these five failures represent a failure rate of 0.00001 for the Permian Basin and 0.00 for the Delaware Basin.

DOE acknowledges the possibility of wells drilled at incorrect locations that were not identified or there may be additional failure modes. Because of these possibilities, DOE increased the failure rate by three orders of magnitude to 0.01 to provide a bounding value for the performance assessment calculation. Appendix PAR of the CCA identifies the parameters FPICD and FPICM as the PIC multiplicative factors for human intrusion by drilling and by mining, respectively. The PIC factors are constants without distributions. Thus, for the performance assessment calculation, DOE considered the PIC to be 0.99 effective in deterring inadvertent human intrusion over the entire withdrawal area for the period of 100-700 years after facility closure.

5.4 PAVT

EPA's consideration of DOE's proposed credit for implementation of the PIC system focused on three questions (EPA, 1997b)

- Did DOE rely on informed judgment, principally expert judgment?
- Is the period of time proposed by DOE for the effectiveness of PIC reasonable?
- Did DOE assume that the PIC eliminates the likelihood of human intrusion?

EPA found that DOE did not conduct an expert judgment process in the manner required by 40 CFR 194.26. Rather, DOE prepared a "credit proposal" that underwent a peer review that, in EPA's judgment, was not equivalent to an elicitation of expert judgment. Also, DOE's documentation of the PIC peer review did not comport with the regulatory requirements because the peer review panel had three members rather than the requisite five called for in 194.26(b)(7)(i).

Furthermore, DOE's peer review was inadequate in that it relied on two expert judgments undertaken prior to promulgation of the final compliance criteria, and neither judgement reviewed the conceptual design for the PIC system nor were the panels requested to derive a credit proposal based on that design. DOE did not attempt, in the CCA, to demonstrate that the judgements complied with the regulations or demonstrate that the proposed credit had been developed. For these reasons, EPA noted that the results of these exercises were not directly relevant to DOE's credit proposal.

EPA found that DOE's proposed credit that the PIC will remain effective over a 600-year period, fell within EPA's limitation that PIC credit could apply no more than approximately 700 years past the time of closure. EPA also found that the credit proposal was consistent with DOE's estimates for the amount of time that the PIC would be expected to endure and be understood

(i.e. well past 700 years).

Regarding the elimination of the likelihood of human intrusion, EPA found that it is highly likely that the proposed PIC will endure for at least 700 years, and it is likely that someone will be able to interpret messages on markers 700 years into the future.

Further, EPA recognized that DOE would need to make assumptions about the future in order to quantify the effectiveness of the PIC over time. However, EPA found that DOE mischaracterized these assumptions as grounded in fact, when at best they are informed predictions. DOE also did not discuss the uncertainties associated with its assumptions, or with the assumptions as a whole. Rather, the assumptions were used to eliminate potential failure scenarios. For instance, DOE concluded that messages and records are virtually certain to be understood by future drillers, simply because DOE assumed that current English will continue to be read by the natural resources exploration and exploitation industries. EPA also agreed with public comments stating that DOE underestimated the potential for PIC to fail to communicate with future generations. DOE did not distinguish between virtual certainty that the PIC will be effective and the assumption that the PIC will entirely eliminate the likelihood of human intrusion. EPA therefore concluded that "virtually certain" was in practical terms equivalent to "certain" as played out in DOE's methodology for quantifying the potential failure rate for PICs (EPA, 1998a).

EPA agreed with DOE that human error in the well drilling regulatory process or in siting a drilling location is the most probable scenario of a human intrusion. However, EPA determined that the uncertainty associated with this failure scenario was probably greater than entertained by DOE, principally because DOE relied on anecdotal information such as informant interviews.

EPA also found that DOE failed to consider another plausible failure scenario involving land controls. The Environmental Evaluation Group (EEG) had documented instances where important DOE documents either inconsistently addressed or overlooked two active leases and a gas well within the WIPP land withdrawal area.

EEG also evaluated the working effectiveness of DOE's Memorandum of Understanding with the U.S. Bureau of Land Management (BLM) that called for BLM to notify DOE of applications to develop resources within one mile of the land withdrawal boundary and wait to issue a permit until DOE had commented. EEG found instances in which BLM or DOE had not followed the procedures established under the Memorandum of Understanding.

Lastly, EEG noted that in 1996 a vertical well was drilled on a lease near the withdrawal area, even though DOE had already purchased the lease in 1978 to prevent resource exploration and exploitation. EPA asserted that these failures of administrative procedures and protocols suggest that government control over the WIPP site can involve error or oversight and should not be assumed to be completely effective.

In conclusion, EPA did not agree with the PIC credit proposed by DOE because (EPA, 1998a):

- DOE's proposed credit did not account for uncertainty in a conservative

manner

- DOE did not employ expert judgment to derive the credit
- DOE's analysis did not account persuasively for the uncertainty associated with forecasting the effectiveness of PIC

The EPA concluded that no credit should be taken for PIC.

The resulting parameter values for the PAVT versus the CCA are shown in Table 5.1

Table 5.1 Multiplicative Factor for Passive Institutional Controls in CCA and PAVT

Parameter Identifier ^(a)	CCA Value	PAVT Value
GLOBAL/FPICD GLOBAL/FPICM	0.01 for 100-700 years	1.0 for 100-700 years

^(a)The material name is listed first followed by the property name.

5.5 CONCLUSION

The converged PA baseline will not include credit for the effectiveness of the PIC design to deter human intrusion into the disposal system, therefore the multiplicative factor will be assigned a value of 1. The resulting parameter values for the RPB are shown in Table 5.2.

Table 5.2. Effectiveness of Passive Institutional Controls in the RPB

Parameter Description	Parameter Identifier ^(a)	Range	Distribution
Effectiveness of Passive Institutional Controls	GLOBAL/FPICD GLOBAL/FPICM	1.0 for 100-700 years	Constant

^(a)The material name is listed first followed by the property name.

6. WASTE SHEAR STRENGTH

6.1 INTRODUCTION

This section documents the type of distribution and range of values selected for the waste shear strength in the RPB. This parameter is implemented as TAUFAIL for the material BOREHOLE. TAUFAIL is the waste shear strength, and is used in the CUTTINGS_S code.

6.2 BACKGROUND

The cavings component of direct surface release consists of that quantity of waste material that is eroded from the borehole wall by the action of the flowing drilling fluid after a waste disposal room is penetrated. The erosion process is assumed to be driven solely by the shearing action of the drilling fluid (mud) on the waste as it moves up the borehole annulus. The state of the waste

material at the time of intrusion by a drill bit is a major factor in the shear resistance to erosion. Since the future states of decomposed waste are both time dependent and uncertain, the resistance to erosion of the waste was treated as a sampled parameter in the CCA.

6.3 CCA

WIPP specific experimental data were not available for the effective shear resistance to erosion of the waste at the time of the CCA. Therefore, the parameter for waste shear strength was estimated conservatively from data for an ocean-bay mud (Parthenaides and Paswell, 1970) or a montmorillonite clay (Sargunam et al., 1973). This resulted in assuming a uniform distribution for the effective shear strength in the borehole with a range from 0.05 to 10 Pa and a median value of 5.0 Pa.

6.4 PAVT

The sensitivity of the cavings model to changes in the waste shear resistance was studied by the EPA as part of their evaluation for the PAVT. They found that the cavings model demonstrated a significant sensitivity to the value chosen for the shear resistance of the waste. The low value chosen for the waste shear resistance was of particular interest to the EPA because a weaker material would result in greater cavings releases. As a result, the EPA required the DOE to change its method for estimating waste shear resistance and use an estimation technique based on particle size distributions instead of using analog experimental data as was done for the CCA.

For the PAVT, the waste shear resistance was estimated based on particle size distributions determined by an expert elicitation panel. The estimate used the Shield's parameter, which relies on a measure of the central point of a population of particles of various sizes, to determine the critical shear stress for an erodible, cohesionless sediment bed (Simon and Senturk, 1992). With this approach, the calculated critical shear stresses ranged from 0.64 Pa to 77 Pa. For conservatism, the low value for waste shear resistance from the CCA PA was retained for the low value in the PAVT while the high value from the Shield's parameter method was used for the high value in the PAVT. The decision to use 0.05 Pa for the low value was supported by information that indicated that very fine-grained materials are not cohesionless as assumed in the Shield's parameter calculation. The information also showed that a lower bound of the critical shear stress for fine-grained cohesive sediments is on the order of the 0.05 Pa. (Parthenaides and Paaswell, 1970) The high end of the range was considered appropriate for cohesionless particles and was retained based on the expert elicitation results. A log uniform distribution for the waste shear resistance was selected for the PAVT to provide equal weighting over the three orders of magnitude in the range, 0.05 to 77 Pa.

The resulting parameter values for the PAVT versus the CCA are shown in Table 6.1.

Table 6.1. Waste Shear Strength in CCA and PAVT

Parameter Identifier ^(a)	CCA Value	PAVT Value
BOREHOLE/TAUFAIL	A uniform distribution from 0.05 to 10 Pa	A log uniform distribution from 0.05 to 77 Pa

^(a)The material name is listed first followed by the property name.

6.5 CONCLUSION

In the CCA, the waste shear strength was estimated conservatively from data for soft mud and non-cohesive sediments, which are not realistic analogues of future states of anticipated WIPP waste and backfill material.

In the PAVT, the EPA changed the CCA assumption of a uniform distribution with a range of 0.05 to 10 Pa to a log-uniform distribution ranging from 0.05 to 77 Pa. While the change to a log-uniform distribution is reasonable, both the upper and lower bound for the range of stress are questionable. The lower value of 0.05 Pa is too low or conservative based on results reported in Jepsen et al. (1998a) for a horizontal flume configuration. Samples tested were MgO and two waste surrogates that were developed by Hansen et al. (1997). Values from the initial work were all greater than 0.2 Pa and the average critical shear stress was 2.6 Pa. In addition, shear stresses lower than 0.2 Pa have never been reported for sediments or quartz particles below the 1 mm surficial layer (Jepsen et al., 1997a and b; 1998a and b; 1999; Roberts et al., 1998). The upper value of 77 Pa is much higher than what is measurable in a laboratory test and therefore cannot be confirmed experimentally. Although the shear stresses in the borehole may be as high as 77 Pa as determined from the cavings conceptual model for helical flow, it is doubtful that any material other than a solid homogenous material such as steel or concrete could withstand this stress.

Further, there is no assumed relationship between waste shear strength and pressure in either the CCA or the PAVT. As the waste is compacted over time the pressure exerted on it will reach a lithostatic value near 2000 psi (1.4×10^7 Pa). As the waste is compacted it is reasonable that its potential for erosion will decrease. Jepsen et al. (1997a) has demonstrated a relationship between density and erosion in sediments.

However, until additional experimental data becomes available, the range of values selected for the PAVT is certainly inclusive of any reasonable values for the shear strength of the waste. Therefore, the technical baseline will adopt the PAVT values until new data are reviewed and approved for use in performance assessment calculations. The resulting parameter values for the RPB are shown in Table 6.2

Table 6.2. Waste Shear Strength in the RPB

Parameter Description	Parameter Identifier ^(a)	Range	Distribution
Critical Waste Shear Strength	BOREHOLE/TAUFAIL	0.05 to 77 Pa	Log-Uniform

^(a)The material name is listed first followed by the property name.

7. ACTINIDE SOLUBILITIES

7.1 INTRODUCTION

This section documents the type of distribution and range of values selected for the coefficient, A, in the equation, $\text{solubility} = A \times 10^b$, for actinide solubilities in the RPB. The coefficients in the solubility equations are implemented as the properties SOLSIM (for solubility in the Salado brine) and SOLCIM (for solubility in the Castile brine) for the materials SOLMOD3, SOLMOD4, SOLMOD5, and SOLMOD6. For example, SOLSIM for the material SOLMOD3 is the coefficient, A, in the solubility equation for all actinides with a +III oxidation state in the Salado brine. Similarly, SOLCIM for the material SOLMOD4 is the coefficient, A, in the solubility equation for all actinides with a +IV oxidation state in the Castile brine. The EPA did not challenge the parameter value for SOLMOD6; EPA challenged the parameter values for the other oxidation state models listed in Table 7.1. The coefficients, A, are used in the PANEL and NUTS codes.

Table 7.1. Definition of the SOLMOD and SOLSIM Parameters

Parameter Identifier ^(a)	Parameter Definition ¹⁾
SOLMOD3/SOLSIM	Coefficient, A, in the solubility equation for all actinides with a +III oxidation state in the Salado brine.
SOLMOD4/SOLSIM	Coefficient, A, in the solubility equation for all actinides with a +IV oxidation state in the Salado brine.
SOLMOD5/SOLSIM	Coefficient, A, in the solubility equation for all actinides with a +V oxidation state in the Salado brine.
SOLMOD3/SOLCIM	Coefficient, A, in the solubility equation for all actinides with a +III oxidation state in the Castile brine.
SOLMOD4/SOLCIM	Coefficient, A, in the solubility equation for all actinides with a +IV oxidation state in the Castile brine.
SOLMOD5/SOLCIM	Coefficient, A, in the solubility equation for all actinides with a +V oxidation state in the Castile brine.

^(a)The material name is listed first followed by the property name.

7.2 BACKGROUND

Actinide solubility parameters play a part in actinide transport from the repository to the surrounding environment, particularly in the event of a direct brine release (DBR) as a result of a human intrusion event. Actinide solubility in Salado brine is of concern in the scenario of drilling intrusion into the repository. Repository pressure could give rise to flow of Salado brine

through the waste and mobilization of actinides. A borehole that passes through the repository may hit a pressurized brine pocket in the Castile formation, resulting in mobilization of actinides in Castile-type brine. Movement of Castile brine through the Salado Formation would result in brine of mixed composition, intermediate between Salado and Castile. Therefore, the solubility of actinides in these brines may be bounded by solubility parameters in each individual brine. In order to adequately model actinide transport in these brines it is necessary to determine the solubility of the actinides in both the Salado and Castile brines.

7.3 CCA

DOE used the the Fracture-Matrix Transport (FMT) computer code to calculate actinide solubility in Castile and Salado brines for the CCA. DOE assumed that chemical conditions in the repository were based on equilibrium between brucite and magnesite and calculated solubilities for three actinides: Am(III), Th(IV), and Np(V). The CCA also required solubilities for Pu(III), U(IV), Np(IV) and Pu(IV), and Pu(V) but insufficient experimental data was available. Consequently, the calculated solubilities for Am(III), Th(IV), and Np(V) were used as analogs for the solubility of Pu(III), U(IV), Np(IV) and Pu(IV), and Pu(V), respectively.

7.4 PAVT

The EPA identified errors in the FMT database used to calculate solubilities in the CCA PA. Upon correction of the FMT database parameters, the EPA published new solubility values for the +III, +IV, and +V oxidation states for radionuclides in Salado and Castile brines. The revised values were used in the PAVT.

The EPA not only identified errors in the FMT database, but the agency also changed assumptions as to which MgO reaction products control pH and partial pressure of CO₂. The DOE assumed chemical conditions based on equilibrium between brucite and magnesite but the EPA chose to assign equilibrium conditions between brucite and hydromagnesite, which buffer at different values of pH and CO₂ partial pressure. The EPA provided results for calculations based on two different hydromagnesite stoichiometries, Mg₅(CO₃)₄(OH)₂•4H₂O and Mg₄(CO₃)₃(OH)₂•3H₂O because they stated that it was not clear which would be prevalent under repository conditions.

The CCA and PAVT values for the solubility parameters are summarized in Table 7.2.

Table 7.2. Actinide Solubility Parameters Used in the CCA and PAVT

Parameter Identifier ^(a)	Radionuclide Oxidation		CCA Value (moles/liter)	PAVT Value (moles/liter)
	State			
SOLMOD3/SOLSIM	+III		5.82×10^{-7}	1.2×10^{-7}
SOLMOD3/SOLCIM	+III		6.52×10^{-8}	1.3×10^{-8}
SOLMOD4/SOLSIM	+IV		4.4×10^{-6}	1.3×10^{-8}
SOLMOD4/SOLCIM	+IV		6.0×10^{-9}	4.1×10^{-8}
SOLMOD5/SOLSIM	+V		2.3×10^{-6}	2.4×10^{-7}
SOLMOD5/SOLCIM	+V		2.2×10^{-6}	4.8×10^{-7}

^(a)The material name is listed first followed by the property name.

7.5 CONCLUSION

EPA identified the parameters listed in Table 7.1 as requiring correction. SNL corrected the database and recomputed actinide solubilities as documented in Novak (1997). EPA accepted these corrected values during their review of the actinide source term used for the CCA (EPA, 1998c). However, the values mandated by EPA for the PAVT do not agree with the recalculated solubilities in the review of the actinide source term. The reason for the discrepancy remains unclear. Consequently, the RPB adopts the values and distributions used in the PAVT as shown in Table 7.3, with the caveat that the discrepancies between the PAVT references will be resolved prior to submittal of any performance assessment results to the EPA.

Table 7.3. Actinide Solubility Parameters in the RPB

Parameter Identifier ^(a)	Radionuclide Oxidation		RPB Value (moles/liter)	Distribution
	State			
SOLMOD3/SOLSIM	+III		1.2×10^{-7}	Constant
SOLMOD3/SOLCIM	+III		1.3×10^{-8}	Constant
SOLMOD4/SOLSIM	+IV		1.3×10^{-8}	Constant
SOLMOD4/SOLCIM	+IV		4.1×10^{-8}	Constant
SOLMOD5/SOLSIM	+V		2.4×10^{-7}	Constant
SOLMOD5/SOLCIM	+V		4.8×10^{-7}	Constant

^(a)The material name is listed first followed by the property name.

8. INUNDATED STEEL CORROSION RATE

8.1 INTRODUCTION

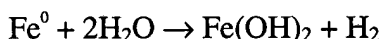
This section documents the type of distribution and range of values selected for the inundated steel corrosion rate in the RPB. This parameter is implemented as CORRMCO2 for the material STEEL. CORRMCO2 is inundated steel corrosion rate, and is used in the BRAGFLO code.

8.2 BACKGROUND

The Transuranic Waste Baseline Inventory Report (TWBIR) (DOE, 1996b) indicates that a large amount of steel in both containers and waste materials will be present in the WIPP repository. Steel can react with the repository brine to form hydrogen gas. Together with microbial gas generation, steel corrosion is expected to have a significant impact on WIPP long-term processes such as brine inflow and room closure by increasing repository gas pressure. Steel corrosion will consume water, and therefore, maintain a reducing environment in the repository, thus affecting actinide behavior.

8.3 CCA

Based on experimental results (Telander & Westerman, 1993; 1997), steel is expected to corrode in the repository via the following reaction (Wang and Brush, 1996a and b):



The rate of this reaction under a brine-inundated condition (no CO₂ present at all) is estimated to be 0 - 0.5 μm/year (0 - 1.59 x 10⁻¹⁴ m/s). This steel corrosion rate was estimated by DOE based on long-term anoxic steel corrosion experiments. Because of its uncertainty, this parameter was treated as a sampled variable in the CCA with a uniform distribution ranging from 0.0 to 1.59 x 10⁻¹⁴ m/s.

8.4 PAVT

The EPA questioned both the upper and lower bounds on DOE's assigned range of values for CORRMCO2. In a simple sensitivity analysis performed by EPA, the lower bound for CORRMCO2 was set to a small but non-zero value to determine if there was any effect on baseline results. They found there was no effect. Therefore, while the EPA did not expect that CORRMCO2 would drop to zero, they believed it could fall to a low value and any change in the low value would have no significant impact on PA modeling results.

When evaluating the upper bound on the range of values DOE assigned to the steel corrosion rate, the EPA carefully examined experimental results that addressed the impact of contact with salt, pH, pressure, and the presence of aluminum. In all cases, except for the case of high pressure, the EPA, like the DOE, concluded that the upper bound for the steel corrosion rate used in the CCA was appropriate.

However, the EPA questioned the upper bound for the steel corrosion rate in the case of high pressures in the repository. Some experiments of six months duration conducted on steel immersed in brine under a hydrogen atmosphere indicated that the steel corrosion rate first decreased at pressures from 2 to 70 atm and then increased at pressures from 70 to 127 atm (Telander and Westerman, 1993). Because the repository may approach or exceed lithostatic pressure and because of the increase in the experimental corrosion rates at higher pressures, the EPA requested that DOE double the upper bound of the inundated corrosion rate in the PAVT to 3.17×10^{-14} m/s.

Table 8.1. Inundated Steel Corrosion Rate in CCA and PAVT

Parameter Identifier ^(a)	CCA Value	PAVT Value
STEEL/CORRMCO2	Uniform distribution from 0 to 1.587×10^{-14} m/s	Uniform distribution from 0 to 3.17×10^{-14} m/s

^(a)The material name is listed first followed by the property name.

8.5 CONCLUSION

The effect of gas pressure on anoxic steel corrosion is not well understood. To capture the possible uncertainty in WIPP performance assessment due to varying steel corrosion rates, it is recommended that the RPB adopt the range of values for the steel corrosion rate used in the PAVT.

Table 8.2. Inundated Steel Corrosion Rate in the RPB

Parameter Description	Parameter Identifier	Range	Distribution
Steel Corrosion Rate	STEEL/CORRMCO2	0 to 3.17×10^{-14} m/s	Uniform

9. MATRIX DISTRIBUTION COEFFICIENTS IN THE CULEBRA

9.1 INTRODUCTION

This section documents the type of distribution and range of values selected for the matrix distribution coefficients, K_{ds} , in the RPB. These parameters are implemented as MKD_AM, MKD_NP, MKD_PU, MKD_TH, and MKD_U for the materials AM(III), NP(IV), NP(V), PU(III), PU(IV), TH(IV), U(IV), and U(VI). For example, MKD_AM for the material AM(III) is the K_d for Americium in the +III oxidation state. The parameters are defined further in Table 9.1. The K_{ds} are used in the SECOTP2D code.

Table 9.1. Definition of the Matrix Distribution Parameters

Parameter Identifier ^(a)	
AM+3/MKD_AM	K_d for Am in the +III oxidation state
NP+4/MKD_NP	K_d for Np in the +IV oxidation state
NP+5/MKD_NP	K_d for Np in the +V oxidation state
PU+3/MKD_PU	K_d for Pu in the +III oxidation state
PU+4/MKD_PU	K_d for Pu in the +IV oxidation state
TH+4/MKD_TH	K_d for Th in the +IV oxidation state
U+4/MKD_U	K_d for U in the +IV oxidation state
U+6/MKD_U	K_d for U in the +VI oxidation state

^(a)The material name is listed first followed by the property name

9.2 BACKGROUND

The Culebra Dolomite of the Rustler Formation presents a potential pathway for migration of actinides to the accessible environment. Therefore the matrix distribution coefficients for the actinides between the aqueous and solid phases are parameters of considerable concern.

9.3 CCA

The matrix distribution coefficient parameter sets for the actinides in the Culebra were developed as a result of experiments at LANL and SNL (Brush, 1996). The K_d values used in the CCA are summarized in the Table 9.2. A uniform distribution over the specified range was assumed for all matrix distribution coefficients.

Table 9.2. Matrix Distribution Coefficient Ranges and Distributions in the CCA

Parameter Description	Parameter Identifier ^(a)	CCA Value	PAVT Value
Matrix Distribution Coefficient for Am(III)	AM+3 /MKD_AM	0.02-0.5 m ³ /kg Uniform	0.02-0.5 m ³ /kg Log Uniform
Matrix Distribution Coefficient for Np(IV)	NP+4/MKD_NP	0.9-20 m ³ /kg Uniform	0.9-20 m ³ /kg Log Uniform
Matrix Distribution Coefficient for Np(V)	NP+5/MKD_NP	0.001 - 0.2 m ³ /kg Uniform	0.001 - 0.2 m ³ /kg Log Log Uniform
Matrix Distribution Coefficient for Pu(III)	PU+3/MKD_PU	0.02-0.5 m ³ /kg Uniform	0.02-0.5 m ³ /kg Log Uniform
Matrix Distribution Coefficient for Pu(IV)	PU+4 /MKD_PU	0.9-20 m ³ /kg Uniform	0.9-20 m ³ /kg Log Uniform
Matrix Distribution Coefficient for Th(IV)	TH+4/MKD_TH	0.9-20 m ³ /kg Uniform	0.9-20 m ³ /kg Log Uniform
Matrix Distribution Coefficient for U(IV)	U+4 /MKD_U	0.9-20 m ³ /kg Uniform	0.9-20 m ³ /kg Log Uniform
Matrix Distribution Coefficient for U(VI)	U+6 /MKD_U	0.00003-0.03 m ³ /kg Uniform	0.00003-0.03 m ³ /kg Log Uniform

^(a)The material name is listed first followed by the property name.

9.4 PAVT

The EPA evaluated the DOE's determination of K_{ds} due to the importance of this parameter in modeling actinide migration in the Culebra (EPA, 1998d). The EPA evaluation included a literature review and comparison of published values with those used by the DOE. In general, the EPA found that DOE assumptions regarding K_{ds} in the CCA were conservative. As a result, the EPA did not ask for a change in the range of values assumed for K_{ds} in the CCA.

The EPA did question the probability distributions assigned to the ranges of the K_d values. The EPA's review of experimental K_d data indicated that K_d values appeared to be logarithmically distributed. In addition, since the actinide K_{ds} ranged over more than an order of magnitude, the EPA felt that a log uniform distribution was more appropriate (EPA, 1998a). The resulting PAVT values and distributions are summarized in Table 9.2.

9.5 CONCLUSION

Subsequent to the PAVT, two errors were found in the procedures used to calculate the matrix K_{ds} after they were submitted for the CCA calculations. First, a brine density of 1.00 g/ml was used rather than the measured brine density, and, second, incorrect values for the mass of dolomite were incorporated (Brush and Storz, 1996). The erroneous use of these values led to incorrectly calculated distribution coefficients. However, the influence of the changes in these values on the distribution coefficients was calculated and reported as minimal (Brush and Storz, 1996). These errors were corrected in the values calculated by Brush and Storz (1996).

For some isotopes, Brush and Storz calculated K_{ds} for both deep (Castile or Salado) and Culebra brines. To remain conservative and consistent with the CCA, the RPB uses the range of K_d values for the brine that has the smaller mean value. Probability distributions for all of the matrix distribution coefficients are log uniform distributions, based upon EPA directives for the PAVT. The matrix distribution coefficients for the RPB are listed in Table 9.3.

Table 9.3. Matrix Distribution Coefficient Ranges and Distributions in the RPB

Parameter Description	Parameter Identifier ^(a)	RPB Value	Probability Distribution
Matrix Distribution Coefficient for Am(III)	AM+3 /MKD_AM	0.02-0.4 m ³ /kg	Log Uniform
Matrix Distribution Coefficient for Np(IV)	NP+4/MKD_NP	0.7-10 m ³ /kg	Log Uniform
Matrix Distribution Coefficient for Np(V)	NP+5/MKD_NP	0.001-0.2 m ³ /kg	Log Uniform
Matrix Distribution Coefficient for Pu(III)	PU+3/MKD_PU	0.02-0.4 m ³ /kg	Log Uniform
Matrix Distribution Coefficient for Pu(IV)	PU+4 /MKD_PU	0.7-10 m ³ /kg	Log Uniform
Matrix Distribution Coefficient for Th(IV)	TH+4/MKD_TH	0.7-10 m ³ /kg	Log Uniform
Matrix Distribution Coefficient for U(IV)	U+4 /MKD_U	0.7-10 m ³ /kg	Log Uniform
Matrix Distribution Coefficient for U(VI)	U+6 /MKD_U	0.00003-0.02 m ³ /kg	Log Uniform

^(a) Values include correction for brine density and mass of dolomite (Brush and Storz, 1996).

10. DRILLING INTRUSION – PROBABILITY OF HITTING A BRINE RESERVOIR

10.1 INTRODUCTION

This section documents the type of distribution and range of values selected for the probability of hitting a brine reservoir during a drilling intrusion in the RPB. The parameter is implemented as PBRINE for the material GLOBAL, and is used in the CUTTINGS_S code.

10.2 BACKGROUND

DOE selected the present site for the WIPP partly based on information obtained from investigations of the underlying geologic and hydrologic systems. In 1975 as part of the program to characterize candidate locations for the then-proposed WIPP, DOE drilled various wells, one of which was designated ERDA-6. The ERDA-6 well began to produce pressurized brine and gas at about 2,711 feet in the Castile Formation. DOE found that ERDA-6 had penetrated increasingly deformed beds as it advanced through the Salado Formation into the Castile Formation. Interpretative analysis at that time found that beds were displaced structurally by as much as 950 feet, and some of the lower beds may have pierced overlying beds. DOE concluded that the beds were too structurally deformed to mine in a reasonable manner along single horizons, therefore the initial site was abandoned.

Beginning in 1977, DOE began to investigate a new site location and drilled WIPP-12 and other wells. WIPP-12 was initially completed in the upper Castile Formation and was later deepened to test for brine and gas in the Castile Formation. At that time DOE considered the probability of encountering brine and gas as relatively low, because ERDA-6 and other known brine reservoirs in the region typically occurred in formations having greater structural deformation. During drilling, however, WIPP-12 began to produce pressurized brine and gas (for additional details see Section 2.1.6.1.1/DOE, 1996a).

Based on these drilling experiences as well as hydraulic tests of the ERDA-6 and WIPP-12 wells, DOE concluded that the Castile Formation is dominated by anhydrite and halite zones of low permeability (DOE, 1997) in which most brine is stored in low permeability microfractures that are oriented vertically or slightly less than vertical. However, fracturing in the anhydrite zone of the upper portion of the formation produced relatively isolated regions with much greater permeability than the surrounding intact anhydrite. These “brine reservoirs” contain brine at greater than hydrostatic pressure. Popielak et al. (1983) estimated the volumes of brine within the reservoirs penetrated by the ERDA-6 and WIPP-12 wells to be 3.5×10^6 and 9.5×10^7 cubic feet, respectively.

In 1987 DOE conducted a time-domain electromagnetic geophysical survey to evaluate the subsurface areas near the WIPP-12 brine reservoir and the proposed location for the waste disposal panels (ETC, 1988) (see Section 2.2.1.2 of the CCA for additional information). The resulting measurements detected a conductor, which DOE interpreted to be the WIPP-12 brine reservoir; they also indicated that similar brine reservoirs might be present within the Castile Formation under a portion of the waste disposal panels.

DOE concluded that the presence of a brine reservoir beneath the repository remained speculative, but could not be ruled out. DOE also concluded that the reservoirs that may exist under the waste panels have a limited extent and interconnectivity, with brine volume consistent with the lower volume estimated from the WIPP-12 brine encounter. DOE therefore evaluated human intrusion scenarios in the performance assessment calculation that included both single human intrusion events and combinations of multiple boreholes that (1) penetrated a pressurized brine reservoir in the underlying Castile Formation, and (2) did not penetrate such a reservoir.

10.3 CCA

For the CCA (Appendix PAR of the CCA), geophysical methods, geological structure analysis, and geostatistical correlation were performed to determine the probability of intersection of a borehole with both the waste disposal region and a pressurized brine reservoir in the Castile formation. DOE estimated that there is a 0.08 probability that any random borehole that penetrates waste at the WIPP also would penetrate an underlying brine reservoir.

During preparation of the CCA, DOE re-examined their time-domain electromagnetic geophysical survey and found that between 10 and 55 percent of the waste panel area may be underlain by relatively conductive units, possibly due to one or more brine reservoirs (Alumbaugh, 1996). The data did not support a means to distinguish boundaries between possible brine reservoirs and non-reservoir areas. As a consequence, DOE assumed that only one reservoir existed below the waste panels.

DOE also mapped the geologic structure of selected units within the Castile and Salado Formations to examine the relationship between identified brine intercepts and evaporite deformation (see Appendix MASS 18.1 and Attachment 18-6 of the CCA). Studies indicated that many of the observed brine encounters in the Delaware Basin were associated with structural deformation in the Castile Formation (e.g. ERDA-6). The mapping exercise reaffirmed DOE's belief that much of the Castile Formation underlying the WIPP site is generally not deformed (and therefore, the likelihood of a brine reservoir beneath the waste panels was expected to be low). However, DOE did not consider the results of this geologic structural analysis in quantifying the probability of a drilling intrusion intersecting a brine reservoir.

DOE then conducted a geostatistical analysis to estimate the probability of drilling into a fractured reservoir in areas overlain by the waste disposal panels (Appendix MASS 18.1 and Attachment 18-6/ DOE 1996a). The analysis was based on 354 drill holes and 27 brine reservoir intercepts within the vicinity of the WIPP. Geostatistical techniques were used to estimate the probabilities that a randomly placed drilling intrusion would encounter pressurized brine in the Castile Formation. The overall probability for the waste panel area was determined to be 0.08 (a probability of 0.08 that a drilling intrusion would intersect a waste panel and penetrate into a underlying, pressurized brine reservoir). This value was selected for the parameter PBRINE in the performance assessment calculation.

10.4 PAVT

EPA reviewed the CCA and supporting documentation and concluded that the parameter PBRINE should be changed from a constant having a value of 0.08 to a uniform distribution represented by a range of 0.01 to 0.60 (median value of 0.305). EPA believes that this range better reflects the uncertainty in the parameter and is a more appropriate representation of the concept of reasonable expectation than the fixed value of 0.08 used by DOE in the CCA (EPA, 1998a).

In reaching its conclusion, EPA considered the possibility that the WIPP-12 brine reservoir may underlie the entire WIPP site and thus the probability of a drilling intrusion encountering the pressurized reservoir could approach certainty (100 percent). This would require the assumption that this reservoir is cylindrical in shape, which EPA considered unlikely because brine resides in vertical or subvertical fractures, and because of the nature of the results from the time domain electromagnetic soundings.

For these reasons, EPA agreed with DOE that there exists a significant uncertainty concerning the magnitude and extent of brine reservoirs beneath the waste panels, but questioned DOE's basis for the probability of encountering such a brine reservoir to be only 8 percent, since other DOE-generated information indicated that this probability could be as high as 60 percent (EPA, 1998a and b).

EPA found that the most direct information on the presence of brine reservoirs was provided by the time domain electromagnetic information, which could be interpreted to indicate that brine reservoirs underlie as much as 55 percent of the repository. EPA also found that these same data could be interpreted to mean that brine reservoirs may underlie as little as 10 percent of the repository.

Using the time domain electromagnetic information, EPA developed probability distributions for four cases involving either random or block models to correlate adjacent measurements, and assumed either the base of the Castile Formation or the base of the Anhydrite III layer in the Castile Formation as the cutoff point above which brine reservoirs may exist (EPA, 1998a and b). EPA found that it made little difference whether the random model or block model was used to characterize correlation between the time domain electromagnetic measurements. However, the simulated probability distributions for encountering brine were highly sensitive to the geologic assumption of whether or not brine reservoirs exist below the bottom of the Anhydrite III layer. Using the base of the Castile Formation Anhydrite Layer III as the lowermost stratigraphic layer below which no brine reservoirs occur, the simulations showed that the area beneath the WIPP containing brine reservoirs varies from one to six percent. However, if the base of the Castile Formation is the lowermost stratigraphic layer below which no brine reservoirs occur, the area of the excavated repository underlain by reservoirs increases to about 35 to 58 percent.

For these reasons, EPA selected one percent as the lower limit and 60 percent as the upper limit for the fraction of the excavated area underlain by brine reservoirs. The upper limit was slightly larger than the largest estimated value for this parameter, but was less than 100% because it was

unreasonable to assume that brine reservoirs must exist. The lower limit was equal to the smallest estimated value and was greater than zero because it was also unreasonable to assume with absolute certainty that a reservoir does not exist. A uniform distribution was mandated because the range of this parameter spans slightly more than an order of magnitude and the use of a uniform distribution conservatively biased the sampling toward the high end.

EPA concluded that the revised (PAVT) distribution sufficiently and accurately increased the probability of brine reservoir occurrence consistent with examined data. Because the increased probability did not impact repository performance (and results were not sensitive to changes in PBRINE), EPA concluded that the original brine reservoir characteristics were acceptable.

The CCA and PAVT values for the probability of hitting a brine pocket are summarized in Table 10.1.

Table 10.1. Probability of Hitting a Brine Pocket in CCA and PAVT

Parameter Identifier ^(a)	CCA Value	PAVT Value
GLOBAL/PBRINE	A constant value for the probability of hitting a brine pocket of 0.08 was used	A uniform distribution for the probability of hitting a brine pocket with values ranging from 0.01 to 0.60 was used

^(a)The material name is listed first followed by the property name.

10.5 CONCLUSION

The Sandia National Laboratories Technical Library and Records Center undertook a key word-based (brine reservoir/Castile/drilling intrusion probability) literature and records search to identify documentation/research that addresses the probability of a drilling intrusion intersecting a brine reservoir in the Castile Formation. Titles of all recent documents (since 1997) identified by the search were reviewed for relevancy; following this, abstracts and/or complete documents were reviewed to determine if information more recent than that cited in the CCA or PAVT was available. The literature and records search and review did not identify new information that would offer further support of, or otherwise refute the distributions and parameter ranges of the probability of intersecting a brine reservoir.

Therefore, the RPB will adopt the PAVT value for the probability of a drilling intrusion intersecting a brine reservoir in the Castile Formation beneath the WIPP, as shown in Table 10.2.

Table 10.2. Probability of Hitting a Brine Pocket in the RPB

Parameter Description	Parameter Identifier ^(a)	Range	Distribution
Probability of Hitting Brine Pocket	GLOBAL/PBRINE	.01 to .60	Uniform

^(a)The material name is listed first followed by the property name.

11. DRILL STRING ANGULAR VELOCITY

11.1 INTRODUCTION

This section documents the type of distribution and range of values selected for the drill string angular velocity in the RPB. The parameter is implemented as DOMECA for the material BOREHOLE, and is used in the CUTTINGS_S code.

11.2 BACKGROUND

The quantity of waste brought to the surface due to an inadvertent penetration of the repository by an exploratory drill bit depends upon three physical processes:

- Cuttings - waste contained in the cylindrical volume created by the cutting action of the drill bit passing through the waste.
- Cavings - waste that erodes from the borehole in response to movement of drilling fluid within the annulus between the drill collars and the borehole wall
- Spallings - waste forced into the drilling fluid due to pressurization of the repository by waste-generated gas. This requires a repository gas pressure that exceeds the hydrostatic pressure of the drilling mud.

The cavings component of direct surface release, after a waste disposal room is penetrated, consists of that quantity of waste material that is eroded from the borehole wall by the action of the flowing drilling fluid. The erosion process model describes the shearing action on the waste by the drilling fluid as it moves up the borehole annulus. The amount of material eroded from the borehole wall is dependent upon the magnitude of the fluid-generated shear stress acting on the wall and the effective shear resistance to erosion of the compacted, decomposed waste. The drill string angular velocity is required to calculate the fluid-generated shear stress. Drill string speeds can vary from 40 to 220 rpm (Austin, 1983, Rechar et al., 1990) when penetrating through salt deposits. The most probable speed is about 70 rpm (Rechar et al., 1990).

11.3 CCA

For the CCA, the DOE had information about the rotational velocities used in current practice when drilling through salt. Using this information, the DOE derived a median value based on a

constructed cumulative distribution of the known, applicable rotational velocities for drilling in salt. The derived median value was 7.8 radians/second. The CCA PA calculation assigned a constant value of 7.8 radians/second to the drill string angular velocity as shown in Table 11.1.

11.4 PAVT

In its review, the EPA found that the data used to derive the median drill string angular velocity encompassed a rather large range of values, from 4.2 to 23 radians/second. Because of this the EPA wondered if the performance assessment model showed sensitivity to variations in drill string angular velocity over this range. The EPA performed a sensitivity analysis over the range of drill string angular velocities and observed a 60% change in cavings releases. As a result, the EPA determined that a constant value for drill string angular velocity did not sufficiently reflect the uncertainty due to the wide range of possible values. The EPA also found that the potential impact on repository performance was sufficient to warrant use of a range of values and required the DOE to treat the drill string angular velocity as a sampled variable with a constructed cumulative distribution with a minimum of 4.2 radians/second, a maximum of 23 radians/second, and a median of 7.77 radians/second. The data were based on a study of current drilling practices in salt, documented in EPA (1998a).

Table 11.1. Drill String Angular Velocity in the CCA and PAVT

Parameter Identifier ^(a)	CCA Value	PAVT Value
BOREHOLE/DOMEGA	A constant value for the drill string angular velocity of 7.8 radians/second was used	A cumulative distribution with a minimum of 4.2, a maximum of 23, and a median of 7.77 radians/second was used

^(a)The material name is listed first followed by the property name.

11.5 CONCLUSION

The Sandia National Laboratories Technical Library and Records Center undertook a key word-based literature and records search to identify documentation/research that addresses the distribution of rotational drill bit velocities for drilling in salt. Titles of all recent documents (since 1997) identified by the search were reviewed for relevancy; following this, abstracts and/or complete documents were reviewed to determine if information more recent than that cited in the CCA or PAVT was available. The literature and records search and review did not identify new information that would offer further support of, or otherwise refute the distributions and parameter ranges discussed above.

Therefore, the RPB will adopt the PAVT range and distribution of values for the drill string angular velocity, as shown in Table 11.2.

Table 11.2. Drill String Angular Velocity in the RPB

Parameter Description	Parameter Identifier	Range	Distribution
Drill String Angular Velocity	BOREHOLE/DOMEGA	4.2 to 23 radians/second	Cumulative Distribution

12. BRINE RESERVOIR PARAMETERS

12.1 INTRODUCTION

This section documents the type of distribution and range of values selected for the Castile Formation brine reservoir rock compressibility and porosity in the RPB. These parameters are implemented as COMP_RCK and POR_BPKT for the material CASTILER. COMP_RCK and POR_BPKT are the rock compressibility and porosity, respectively, and are used in the BRAGFLO code.

12.2 BACKGROUND

High-pressure brine reservoirs have been encountered in the Castile Formation in boreholes such as WIPP-12 in the controlled area, and ERDA-6 northeast of the site. DOE concluded that the presence of a brine reservoir beneath the repository remained speculative, but could not be ruled out, based on geophysical and geohydrological surveys and other information and analyses. DOE therefore evaluated human intrusion scenarios in the performance assessment calculation that included both single human intrusion events and combinations of multiple boreholes that either penetrated a pressurized brine reservoir in the underlying Castile Formation, or did not penetrate such a reservoir.

DOE determined that, as opposed to aquifers, brine reservoirs in the Castile Formation behave as bounded systems. The potential effect on repository performance of intersecting a brine reservoir during a drilling intrusion was dependent on other reservoir properties – brine reservoir pressure, permeability, compressibility, total brine volume, and porosity. These properties were treated stochastically in the performance assessment calculation.

In the PAVT, EPA required further review of the distributions and range of values for brine reservoir compressibility and brine reservoir volume. EPA found that brine reservoir volume could be estimated more appropriately through simultaneous sampling of rock compressibility and a newly defined parameter, brine reservoir porosity, which was not a parameter considered in the CCA. These parameters are examined more closely in the following sections.

12.3 CCA

12.3.1 Brine Reservoir Rock Compressibility

This parameter, identified as COMP_RCK in the CCA, represents the rock compressibility of the Castile Formation brine reservoir. Rock compressibility is used to calculate the pore compressibility, which in turn is used in BRAGFLO to estimate brine and gas flow within the repository and the Castile Formation.

Parameter values were based on an analysis of data from WIPP-12 (Appendix MASS and MASS Attachment 18-2, and Appendix PAR, Parameter 29). DOE determined rock compressibility values by calculating the bulk modulus of anhydrite from the acoustic log of the Castile Anhydrite III unit found in WIPP-12. DOE chose to use the acoustic log because it measures compressive wave travel time over short distances through relatively intact, undisturbed rock, then uses a correlation between wave velocity and elastic rock properties to estimate bulk modulus. Various laboratory compression tests on anhydrite from other WIPP locations produced similar results for the bulk modulus (Popielak et al., 1983).

The estimated bulk modulus (K) for the intact Anhydrite III at WIPP-12 was 6.9×10^{10} Pa. Assuming uniaxial strain the rock compressibility (C_R) can be estimated from the bulk modulus and the shear modulus (G) of the rock:

$$C_R = \frac{1}{K + \frac{4}{3}G}$$

No estimates for shear modulus of the Anhydrite III layer were available, however, Beauheim et al. (1991) reported a value for shear modulus that was about one-third of the bulk modulus for the Salado Formation anhydrite, that is, $G = 1/3 K$. Based on this estimate, the calculated intact rock compressibility was $1 \times 10^{-11} \text{ Pa}^{-1}$.

Fractured rock may have a bulk modulus 2 to 10 times lower than that of intact rock (Popielak et al., 1983), and a correspondingly higher compressibility. Beauheim et al. (1991) estimated that fracturing might result in a four-fold increase in rock compressibility. DOE therefore reported that rock compressibility could range from $2 \times 10^{-11} \text{ Pa}^{-1}$ to $1 \times 10^{-10} \text{ Pa}^{-1}$.

DOE also reported the results from hydraulic testing in the disturbed Salado Formation anhydrite and halite and found that rock compressibility ranged from $5 \times 10^{-12} \text{ Pa}^{-1}$ to $3 \times 10^{-9} \text{ Pa}^{-1}$ in these zones. Freeze and Cherry (1979) reported a range for rock compressibility for fractured or jointed rock of 1×10^{-8} to 10^{-10} Pa^{-1} .

Given the above, DOE determined that a triangular distribution of the logarithm of the rock compressibility was appropriate for inclusion in the CCA. The distribution had the following statistics:

Minimum – -11.30 log Pa⁻¹
Maximum – -8 log Pa⁻¹
Mode – -10 log Pa⁻¹

DOE selected a log-triangular distribution because the range of values spanned several orders of magnitude, and little was known about the distribution's specific shape, and the midrange values were more likely than the extreme bounding values. DOE established a relatively broad range to ensure that all possible values were encompassed.

12.3.2 Brine Reservoir Pore Volume

This parameter, identified as VOLUME in the CCA, represents the volume of brine that could be produced from a reservoir based primarily upon the reservoir's rock compressibility characteristics. The estimate of volume also considers the interconnectivity of a fractured reservoir, the radii of reservoirs, and the effects of drilling over the 10,000-year period of regulatory interest.

DOE analyzed information from the WIPP-12 borehole to estimate the effective radius of reservoirs and concluded that the reservoirs could range in extent from several hundred meters, which is about the size of a waste panel, to several kilometers. Geophysical survey data generally supported these ranges (Section 6.4.12.6/DOE, 1996a). However, after considering the effective radius as well as the types, configuration, and extent of fracturing, DOE determined that brine reservoirs, which might exist under the waste panels, were limited in extent and interconnectivity, and likely would contain brine volumes consistent with the lower values estimated from WIPP-12.

Brine reservoir pressure is partially depleted upon intersection by a borehole. DOE postulated two conceptual models consistent with this drilling rate and the depletion of brine reservoir pressure:

- Reservoirs would be interconnected over large areas and penetrated and partially depleted many times, and
- Reservoirs would be interconnected over smaller areas and would not be affected by the penetrations that occur outside, yet near the waste-area "footprint."

As noted above, DOE considered the brine reservoirs to be poorly interconnected hydraulically, and further concluded they would be unaffected by penetrations occurring outside but near the waste-area footprint. Reservoirs that could persevere unaltered until intersected offer potentially greater consequences than a depleted, yet larger reservoir, making this a conservative assumption.

The brine volume used in the performance assessment calculation to determine the consequence of the first penetration of a brine reservoir was initially determined to be 32,000 m³, which is the minimum pore volume from the WIPP-12 analysis. However, DOE also considered larger volumes in the calculation - 64,000, 96,000, 128,000 and 160,000 m³, because the WIPP-12

reservoir volume represented an estimated effective area of about one-third the size of a waste panel and because a brine reservoir larger than that encountered at WIPP-12 could exist (Appendix MASS, Section MASS.18, and MASS Attachment 18-3/DOE, 1996a). The volume of the brine reservoir in the CCA calculations was determined by sampling an index parameter, GRIDFLO, which yielded a volume of brine after applying a porosity correction factor.

12.4 PAVT

12.4.1 Brine Reservoir Rock Compressibility

EPA reviewed the CCA, and supporting information and references, and concluded that DOE's compressibility parameter for the Castile Formation brine reservoir was not consistent with available information (EPA, 1998b). Subsequent to the CCA, DOE re-examined the field test data for the WIPP-12 borehole and arrived at a revised range for rock compressibility. EPA regarded the DOE's re-analysis as a better estimate of the rock compressibility parameter than the value used in the CCA. Consequently, EPA required DOE to continue to treat rock compressibility as a sampled variable having a triangular distribution and a revised range of 2×10^{-11} to $1 \times 10^{-10} \text{ Pa}^{-1}$ and a revised mode of $4 \times 10^{-11} \text{ Pa}^{-1}$.

12.4.2 Brine Reservoir Pore Volume

At the time of the PAVT, DOE did not communicate clearly to EPA the method by which brine reservoir pore volume was calculated in the CCA. Consequently, EPA mandated a different method for calculating this value. EPA (1998a) required DOE to include a parameter for the porosity of the rock containing the brine reservoir (POR_BPKT) that could be sampled simultaneously with rock compressibility. Porosity was to have a triangular distribution, with a range of 0.1848 to 0.9240, and a mode of 0.3696. These statistics for the porosity distribution were drawn from a reanalysis of the WIPP-12 data and correspond to a range from 3.4×10^6 to $1.7 \times 10^7 \text{ m}^3$ of brine with an mode of $6.8 \times 10^6 \text{ m}^3$. EPA concluded that a triangular distribution was appropriate because an intermediate value was more likely to occur than either extreme, and because it retains a simple shape that reflects the uncertainty about the distribution's specific shape.

EPA concluded that these changes, in effect, would model the characteristics of the Castile Formation brine reservoirs in the PAVT after those of the WIPP-12 brine reservoir. The parameter changes in the PAVT reduced the rock compressibility range and mode to more appropriate values, and increased the brine reservoir volume. The reduction in compressibility would tend to reduce the reservoir's capability to release brine, while the increased volume would tend to increase that capability. Because the volume increase was substantially greater than the compressibility reduction, the net effect was anticipated to be a "conservative" increase in the brine volume available to flow from the reservoir.

Consequently, instead of sampling over a distribution of brine reservoir volumes as in the CCA, in the PAVT EPA required DOE to calculate the brine reservoir pore volume as the product of the volume of rock in the Castile formation beneath the repository and the brine pocket porosity.

The CCA and PAVT values for the brine reservoir parameters are summarized in Table 12.1.

Table 12.1. Brine Reservoir Parameters in the CCA and PAVT

Parameter Identifier ^(a)	CCA	PAVT
CASTILER/COMP_RCK	Triangular Distribution of logarithm Minimum – $-11.30 \log \text{Pa}^{-1}$ Maximum – $-8 \log \text{Pa}^{-1}$ Mode – $-10 \log \text{Pa}^{-1}$	Triangular Distribution of actual values Minimum – $2 \times 10^{-11} \text{Pa}^{-1}$ Maximum – $1 \times 10^{-10} \text{Pa}^{-1}$ Mode – $4 \times 10^{-11} \text{Pa}^{-1}$
CASTILER/POR_BPKT	Not used in the CCA ^(b)	Triangular Distribution Minimum – 0.1848 Maximum – 0.9240 Mode – 0.3696

^(a)The material name is listed first followed by the property name. ^(b)The CCA determined pore volume by sampling an index parameter GRIDFLO

12.5 CONCLUSION

The Sandia National Laboratories Technical Library and Records Center undertook a key word-based (Castile rock compressibility, Castile porosity, Castile brine volume) literature and records search to identify documentation/research that addresses the three parameters – brine reservoir rock compressibility, porosity, and pore volume. Titles of all recent documents identified by the search were reviewed for relevancy; following this, abstracts and/or complete documents were reviewed to determine if information more recent than that cited in the CCA or PAVT was available. The literature and records search and review did not identify new information that would offer further support of, or otherwise refute the distributions and parameter ranges presented above.

Therefore, the RPB will adopt the range and distributions of brine reservoir parameters as in the PAVT, which are shown in Table 12.2. Brine pocket pore volume will be calculated as the product of the total Castile volume in BRAGFLO, and the sampled porosity of the Castile Formation brine reservoir.

Table 12.2. Brine Reservoir Parameters in the RPB

Parameter Description	Parameter Identifier	Range	Distribution
Brine Reservoir Rock Compressibility	CASTILER/COMP_RCK	2×10^{-11} to $1 \times 10^{-10} \text{Pa}^{-1}$ Mode of 4×10^{-11}	Triangular
Brine Reservoir Porosity	CASTILER/POR_BPKT	0.1848 to 0.9240 Mode of 0.3696	Triangular

13. WASTE UNIT FACTOR

13.1 INTRODUCTION

This section documents the type of distribution and range of values selected for the waste unit factor in the RPB. The parameter is implemented as (WUF) for the material BOREHOLE, and is used in the CCDFGF code.

13.2 BACKGROUND

The parameter WUF, also referred to as "Waste Unit Factor" and as the "Unit of Waste," is defined in the CCA as the number of millions of curies of alpha-emitting transuranic (TRU) radionuclides with half-lives longer than 20 years destined for disposal in the WIPP repository (DOE, 1996a). For brevity, this text refers to such radionuclides as WUF radionuclides. The WUF is used to calculate inventory and release limits based on the requirements promulgated by the EPA at 40 CFR Part 191. In 40 CFR Part 191, the release limits are established as the number of curies of each radionuclide per million curies of WUF radionuclides in the repository. The release limits for some WUF radionuclides are listed in Table 13.1. For example, for every million curies of WUF radionuclides disposed in WIPP, 100 curies of Am-241 can be released over the 10,000 year regulatory timeframe. Therefore, in order to compare repository performance to the standard set in 40 CFR Part 191, the WUF must be estimated and the release limit calculated for each radionuclide.

Table 13.1. Radionuclide Release Limits from 40 CFR 191

Radionuclide	Release Limit in curies per Million Curies of WUF Radionuclides
Am-241 or 243	100
C-14	100
Cs-135 or 137	1000
I-129	100
Np-237	100
Pu-238, 239, 240, 242	100
Ra-226	100
Sr-90	1000
Tc-99	10000
Th-230 or 232	10
Sn-126	1000
U-233, 234, 235, 236 or 238	100
Any other α -emitting radionuclide with a half-life greater than 20 years	100
Any other radionuclide with a half-life greater than 20 years that does not emit α -particles	1000

13.3 CCA

For the CCA, radionuclide inventories that contributed to the WUF were reported in the Transuranic Waste Baseline Inventory Report, Revision 3 (DOE, 1996b). The radionuclides that contributed most to the total waste inventory for the CCA are presented in Table 13.2. The waste unit factor used in the 1996 CCA was 4.07 (i.e. 4.07 million curies). This WUF was calculated from the expected 1995 inventory as shown in Table 13.2.

Table 13.2. WIPP Radionuclide Inventory from the CCA

Radionuclide	Expected 1995 Inventory (curies)	% of WUF
Am-241	4.48×10^5	1.10×10^1
Am-243	3.26×10^1	8.01×10^{-4}
Cf-249	6.87×10^{-1}	1.69×10^{-6}
Cf-251	3.78×10^{-3}	9.28×10^{-6}
Cm-243	1.08×10^2	2.50×10^{-3}
Cm-245	1.15×10^2	2.82×10^{-3}
Cm-246	1.02×10^{-1}	2.51×10^{-6}
Cm-247	3.21×10^{-9}	7.88×10^{-14}
Cm-248	3.69×10^{-2}	9.1×10^{-7}
Np-237	5.64×10^1	1.39×10^{-3}
Pu-238	2.61×10^6	6.41×10^1
Pu-239	7.95×10^5	1.95×10^1
Pu-240	2.15×10^5	5.28×10^0
Pu-242	1.17×10^3	2.87×10^{-2}
Pu-244	1.50×10^{-6}	3.68×10^{-11}
Total	4.07×10^6	9.992×10^1

13.4 PAVT

For the PAVT, the WUF was calculated based on the projected inventory in 2033, the year that WIPP will close. Hence, the WUF was changed to 3.44.

13.5 CONCLUSION

Since the CCA, there are two changes to the WUF that should be included in the RPB (Sanchez, 1996a and b; 1997). The first change includes the addition of the supplementary Savannah River site inventory, and the second change is to the year to which the inventory is decayed. Incorporating these changes results in a WUF value of 3.59 for the RPB.

Since the time of the certification, DOE has determined that some waste at the Savannah River Site (SRS) was not included in the TWBIR, the basis for the CCA and PAVT inventories. The missing SRS waste is rich in ^{238}Pu , ^{230}Th , and ^{234}U as shown in Table 13.3. If the additional SRS inventory is included in the calculation of the WUF, the value (decayed to 1995 values) would be 4.27.

Table 13.3. Additional Inventory Contributions from the Savannah River Site

Radionuclide	Expected 1995 Inventory from TWBIR Rev 3 (Ci)	Expected 1995 Inventory Missing from TWBIR Rev 3 (Ci)	Updated Expected 1995 Inventory (Ci)
Pu-238	2.61×10^6	2.01×10^5	2.81×10^6
U-234	5.08×10^2	1.5×10^1	5.23×10^2
Th-230	8.82×10^{-2}	1.66×10^{-3}	8.99×10^{-2}
Total Expected 1995 Inventory	4.07×10^6		4.27×10^6

The second change resolves the year to which the waste inventory is decayed. In the CCA, the WUF was calculated by adding the current inventory estimate (decayed to 1995) and an estimate of waste to be generated between 1995 and 2033. However, many radionuclides in the current and projected inventory have half-lives that are sufficiently short such that measurable decay, and consequent inventory reduction, will occur between the years 1995 and the projected closing date of 2033. As a result, a WUF that is based on decay to the year 1995 will be significantly larger than one based on decay to the year 2033. A larger value for the WUF results in higher release limits for each radionuclide. Therefore, a WUF based on decay to 2033 is more conservative than a WUF based on decay to 1995, since release limits for each radionuclide are lower.

Therefore, for the RPB, the DOE proposes to calculate WUF using 2033 values for the radionuclide inventories. Sanchez (1997) calculated the 2033 WUF value (including the missing SRS waste) to be 3.59.

14. REFERENCES

Alumbaugh, D.L. 1996. "Re-analysis of the Time Domain Electromagnetic (TDEM) Data Collected at the WIPP Site." ERMS #245405. Sandia National Laboratories. Albuquerque, NM.

Austin, E.H. 1983. *Drilling Engineering Handbook*. International Human Resources Development Corporation. Boston, MA.

Beauheim, R.L. 1996. "Salado Package #16, (X, Y, Z) DRZ Permeability." Revision 1. Records Package. ERMS #232038. Sandia National Laboratories. Albuquerque, NM.

Beauheim, R.L., Saulnier, G.J., Jr., and Avis, J.D. 1991. *Interpretation of Brine-Permeability Tests of the Salado Formation at the Waste Isolation Pilot Plant: First Interim Report*. SAND90-0083. ERMS #226003. Sandia National Laboratories. Albuquerque, NM.

Brush, L.H. 1996. "Ranges and Probability Distributions of K_{ds} for Dissolved Pu, Am, U, Th and Np in the Culebra for the PA Calculations to Support the WIPP CCA" *Memorandum from L.H. Brush to M.S. Tierney, 6/10/96*. ERMS #238801. Sandia National Laboratories. Albuquerque, NM.

Brush, L.H. and Storz, L. 1996. "Revised Ranges and Probability Distributions of K_{ds} for Dissolved Pu, Am, U, Th, and Np in the Culebra for the PA calculations to Support the WIPP CCA" *Memorandum from L.H. Brush to M.S. Tierney, 7/24/96*. ERMS #241561. Sandia National Laboratories. Albuquerque, NM.

Butcher, B.M. 1989. *WIPP Simulated Waste Composition and Mechanical Properties*. SAND89-0372. Sandia National Laboratories. Albuquerque, NM.

Butcher, B.M. 1990. "Disposal Room Porosity and Permeability Values for Disposal Room Performance Assessment" *Memorandum to M.G. Marietta*. Included in SAND89-2408. Sandia National Laboratories. Albuquerque, NM.

Christensen, C.L. and Hunter, T.O. 1980. *The Bell Canyon Test Results*. SAND80-2414C. Sandia National Laboratories. Albuquerque, New Mexico.

DOE (U.S. Department of Energy). 1996a. *Title 40 CFR Part 191 Compliance Certification Application for the Waste Isolation Pilot Plant*. DOE/CAO-1996-2184. U.S. Department of Energy. Carlsbad, NM.

DOE (U.S. Department of Energy). 1996b. *Transuranic Waste Baseline Inventory Report (Revision 3)*. DOE/CAO-95-1121. U.S. Department of Energy. Carlsbad, NM

DOE (U.S. Department of Energy). 1997. *Waste Isolation Pilot Plant Disposal Phase Final Supplemental Environmental Impact Statement*. DOE/EIS-0026-S-2. U.S. Department of Energy. Carlsbad, NM.

EPA (U.S. Environmental Protection Agency). 1997a. *Technical Support Document for Section 194.23:Parameter Justification Report*. Docket No. A-93-02, III-B-14, U.S. Environmental Protection Agency. Washington D.C.

EPA (U.S. Environmental Protection Agency). 1997b. *Compliance Application Review Documents for the Criteria for the Certification and Re-Certification of the Waste Isolation Pilot Plant's Compliance with the 40 CFR Part 191 Disposal Regulations: Proposed Certification Decision*. Docket No. A-93-02, III-B-2. U.S. Environmental Protection Agency. Washington D.C.

EPA (U.S. Environmental Protection Agency). 1998a. *Technical Support Document for Section 194.23:Parameter Justification Report*. Docket No. A-93-02, V-B-14. U.S. Environmental Protection Agency. Washington, D.C.

EPA (U.S. Environmental Protection Agency). 1998b. *Response to Comments, Criteria for the Certification and Recertification of the Waste Isolation Pilot Plant's Compliance with 40 CFR 191 Disposal Regulations: Certification Decision*. Docket No. A-93-02, V-C-1. U.S. Environmental Protection Agency. Washington D.C.

EPA (U.S. Environmental Protection Agency). 1998c. *Technical Support Document for Section 194.24: EPA's Evaluation of DOE's Actinide Source Term*. Docket No. A-93-02, V-B-17. U.S. Environmental Protection Agency. Washington D.C.

EPA (U.S. Environmental Protection Agency). 1998d. *Technical Support Document for Section 194.14: Assessment of K_{ds} Used In The CCA*. Docket A-93-02, Item V-B-4. U.S. Environmental Protection Agency. Washington D.C.

ETC (Earth Technology Corporation). 1988. *Final Report for Time Domain Electromagnetic (TDEM) Surveys at the WIPP Site*. SAND87-7144. ERMS #225668. The Earth Technology Corporation, Golden, CO; Sandia National Laboratories. Albuquerque, NM.

Freeze, R.A. and Cherry, J.A. 1979. *Groundwater*. Prentice-Hall Inc. Englewood Cliffs, New Jersey.

Froehlich, G. 1997. "PAV1 Parameter Values." *Memorandum to C. Lattier*. ERMS #246087. Sandia National Laboratories. Albuquerque, NM.

Hadgu, T. 1999. "Modifications to the 96 CCA Direct Brine Release Calculations." *Memorandum to M. Marietta*. ERMS # 511276. Sandia National Laboratories. Albuquerque, NM.

Hansen, F.D., Knowles, M.K., Thompson, T.W., Gross, M., Schatz, J.F., and McLennan, J. 1997. *Description and Evaluation of a Mechanistically Based Model for Spall at the Waste Isolation Pilot Plant*. SAND97-1369. Sandia National Laboratories. Albuquerque, NM.

Howarth, S.M. 1996. "[Salado Package #13], Salado Anhydrite Permeability in the X-Direction." Records Package. ERMS #230603. Sandia National Laboratories. Albuquerque, NM.

Howarth, S.M., and Christain-Frear, T. 1996. *Porosity, Single-Phase Permeability, and Capillary Pressure Data from Preliminary Laboratory Experiments on Selected Samples from Marker Bed 139 at the Waste Isolation Pilot Plant*. SAND94-0472 (Draft). ERMS 238367. Sandia National Laboratories. Albuquerque, NM.

Jepsen, R., Roberts, J., and Lick, W. 1997a. "Effects Of Bulk Density On Sediment Erosion Rates." *Water, Air, and Soil Pollution*, 99, 21-31.

Jepsen, R., Roberts, J., and Lick, W. 1997b. *Long Beach Harbor Sediment Study*. Report to the U.S. Army Corps of Engineers. Los Angeles District.

Jepsen, R., Roberts, J., and Lick, W. 1998a. "Progress Report: Development And Testing Of Waste Surrogate Materials For Critical Shear Stress, September 1998." *Disposal Room Processes*. ERMS #249064. Sandia National Laboratories. Albuquerque, NM.

Jepsen, R., Roberts, J., and Lick, W. 1998b. *New York Harbor Sediment Study*. Report to the U.S. Army Corps of Engineers. New York District.

Jepsen, R., Roberts, J., and Lick, W. 1999. *Grand River Sediment Study*. Report to the Environmental Protection Agency. Great Lakes District.

Luker, R.S., T.W. Thompson, and Butcher, B.M. 1991. "Compaction and Permeability of Simulated Waste." *In Rock Mechanics as a Multidisciplinary Science: Proceedings of the 32nd U.S. Symposium, University of Oklahoma, Norman, OK, July 10-12, 1991, J.C. Roegiers, ed.* SAND90-2368C. Sandia National Laboratories. Albuquerque, NM.

Novak, C.F. 1997. "Calculation of Actinide Solubilities in WIPP SPC and ERDA 6 Brines under MgO Backfill Scenarios Containing either Nesquehonite or Hydromagnesite as the Mg-CO₃ Solubility-Limiting Phase." *Memorandum of Record to R.V. Bynum, 04/21/97*. ERMS #246124. Sandia National Laboratories. Albuquerque, New Mexico.

Parthenaides, E. and Paswell, R.E. 1970. "Erodibility of Channels with Cohesive Boundary." *Proceedings of the American Society of Civil Engineers, Journal of the Hydraulics Division*. Vol. 96, No. HY3, 755: 771. ERMS #231536.

Popielak, R.S., Beauheim, R.L., Black, S.R., Coons, W.E., Ellingson, C.T., and Olsen, R.L. 1983. *Brine Reservoirs in the Castile Formation, Waste Isolation Pilot Plant (WIPP) Project, Southeastern New Mexico*. TME 3153. U.S. Department of Energy, Waste Isolation Pilot Plant, Albuquerque, NM.

- Rechard, R.P., Iuzzolino, H., and Sandha, J.S. 1990. *Data Used in Preliminary Performance Assessment of the Waste Isolation Pilot Plant (1990)*. SAND89-2408. Sandia National Laboratories. Albuquerque, NM.
- Roberts, J., Jepsen, R., and Lick, W. 1998. "Effects Of Particle Size And Bulk Density On Erosion Of Quartz Particles." *Journal of Hydraulic Engineering*, ASCE, 124(12), 1261-1267.
- Sanchez, L. 1996a. *Justification for Choice of CCA Radionuclide Values*. ERMS #237428. Sandia National Laboratories. Carlsbad NM.
- Sanchez, L. 1996b. *Identification of Important Radionuclides Used in 1996 CCA WIPP Performance Assessment*. ERMS #237431. Sandia National Laboratories. Carlsbad, NM.
- Sanchez, L. 1997. *Recalculation of Waste Unit Factor with the Corrected Radionuclide Inventory*. ERMS #247544. Sandia National Laboratories. Carlsbad NM.
- Sandia WIPP (Sandia National Laboratories). 1991. *Preliminary Comparison with 40 CFR 191, Subpart B for the Waste Isolation Pilot Plant, December 1991*. SAND91-0893/3. Sandia National Laboratories. Albuquerque, NM.
- Sargunam, A., Riley, P., Arulanandan, K., and Krone, R.B. 1973. "Physico-Chemical Factors in Erosion of Cohesive Soils." *Proceedings of the American Society of Civil Engineers, Journal of the Hydraulics Division*. Vol. 99. No. HY3: 555-558.
- Simon, D.B. and Senturk, F. 1992. "Sediment Transport Technology Water and Sediment Dynamics." *Water Resource Publication*.
- Telander M. R. & Westerman, R.E. 1993. *Hydrogen Generation by Metal Corrosion in Simulated Waste Isolation Pilot Plant Environments: Progress Report for the Period November 1989 through December 1992*. SAND92-7347. Sandia National Laboratories. Albuquerque, NM.
- Telander M. R. & Westerman, R.E. 1997. *Hydrogen Generation by Metal Corrosion in Simulated Waste Isolation Pilot Plant Environments*. SAND96-2538. Sandia National Laboratories. Albuquerque, NM.
- Thompson, T.W. and Luker, R.S. 1990. *Compactions and Permeability of Simulated Waste*. SAIC Report for Sandia National Laboratories. Albuquerque, NM
- Thompson, T.W., Coons, W.E., Krumhansl, J.L., and Hansen, F.D. 1996. *Inadvertent Intrusion Borehole Permeability*. Final Draft. Sandia National Laboratories. Carlsbad, NM.
- Tierney, M. 1990. *Constructing Distributions of Uncertain Variables in Models of the Performance of the Waste Isolation Pilot Plant: The 1990 Performance Simulations*. SAND90-2510. Sandia National Laboratories. Albuquerque, NM.

Tisinger, S. 2001. "Changes in CCA Parameter Values Due to Data Cleansing" *Memorandum to Palmer Vaughn*. Sandia National Laboratories. Carlsbad, NM.

Vaughn, P., Bean, J., Garner, J., Lord, M., MacKinnon, R., McArthur, D., Schreiber, J., and Shinta, A. 1995. *FEPs Screening Analysis DR2, DR3, DR6, DR7, and S6*. Record packaged submitted to SWCA-A:1.1.6.3:PA:QA:TSK:DR2, DR3, DR6, DR7, and S6. Sandia National Laboratories. Albuquerque, NM.

Wang Y., and Brush L. H. 1996a. "Estimates Of Gas-Generation Parameters For The Long-Term WIPP Performance Assessment" *Memorandum to M. Tierney, 1/26/1996*. ERMS#231943. Sandia National Labs. Albuquerque, NM.

Wang Y., and Brush L. H. 1996b. "Modify The Stoichiometric Factor Y In The BRAGFLO To Include The Effect Of MgO Added To WIPP Repository As A Backfill". *Memorandum to M. Tierney, 2/23/1996*. ERMS#232286. Sandia National Labs. Albuquerque, NM.